NASA Technical Paper 1534

Preliminary Design Procedure for Insulated Structures Subjected to Transient Heating

Howard M. Adelman

DECEMBER 1979

NASA

NASA Technical Paper 1534

Preliminary Design Procedure for Insulated Structures Subjected to Transient Heating

Howard M. Adelman
Langley Research Center
Hampton, Virginia

National Aeronautics
and Space Administration

**Scientific and Technical
Information Branch**

1979

SUMMARY

A procedure is described for obtaining minimum-mass designs of insulated composite structural panels. The panels are characterized as consisting of a structural layer and an insulation layer. The panels are loaded by a general set of inplane forces applied to the structural layer and a time-dependent temperature applied to the outer surface of the insulation layer. Temperature and stress histories in the panel are given by closed-form solutions, and optimization of the insulation and structural thicknesses is performed by nonlinear mathematical programming techniques. Design constraints are enforced at a finite number of discrete times over the time period of interest, and satisfactory results are obtained with a small number of times.

The computerized procedure is intended for preliminary design calculations to evaluate materials for specified applications and to perform parameter studies. A set of design calculations is presented to evaluate the efficiency of the following eight structural materials under combined heating and mechanical loads: graphite/polyimide (Gr/PI), graphite/epoxy (Gr/E), boron/aluminum (B/Al), titanium (Ti), aluminum (Al), Rene 41, carbon/carbon, and Lockalloy. A study is also performed to assess the effect on design mass of the intensity and duration of heating for the eight materials. Examinations of final designs indicate that, for sufficiently high mechanical loads, an optimum structure has a temperature response well below the recommended allowable temperature for the material. A comparison of these designs with those assumed to operate at the allowable temperatures indicates that significant mass savings may be attainable by the lower temperature operation.

INTRODUCTION

A current technical challenge in the design of high-speed flight vehicles is the development of optimum structural design concepts for combined heating and mechanical loading applications. A concept of interest for applications to atmospheric reentry vehicles is the insulated configuration in which the structure is protected from heating by insulation placed between the airstream and the structure. The potential benefits of structural concepts composed of fiber-reinforced composite materials are currently being evaluated (ref. 1). At an early stage in the design of such thermal-structural concepts, it is beneficial to conduct selected design studies to (1) evaluate candidate structural and insulation materials to narrow the choice of materials to a small number of contenders and (2) obtain a preliminary estimate of the optimum combination of structural and insulation material. An emerging philosophy for conducting such studies is integrated thermal-structural analysis and design (refs. 2 to 4) in which all important interactions between the thermal and structural responses of the structure are properly accounted for at every stage in the design process. Presented herein is a design technique to define the best combination of insulation and structural thicknesses which minimizes the total mass under a specified set of inplane mechanical loads and a transient heating pulse.

Previous investigators have addressed the minimum-mass design of insulated structures (refs. 5 to 8), but consideration has been limited to metallic structures, uniaxial loading, and a restricted class of heating pulses. These simplifications were needed since the classical minimization techniques required extensive manipulations of algebraic equations.

In the present work the structure considered is either a metal layer or a composite laminate under a general set of inplane mechanical loads and heating pulse. This generalization is facilitated by the use of nonlinear mathematical programming techniques to generate the designs systematically. An important aspect of the present approach is the treatment of the requirement that time-dependent temperatures and stresses be less than specified allowable values for all appropriate values of time. This aspect has received relatively little attention. In reference 9, which deals with the optimization of an ablating heat shield, constraints on time-dependent temperatures and stresses are replaced by time-integrated averages of the original constraints. The integrals are carefully formulated to avoid constraint violations, but, as pointed out in reference 9, the integral representation of the constraints leads to a smoothing effect which causes temperatures and stresses to be somewhat insensitive to changes in the structural size parameters. The approach used in the present work is a simple time slicing in which the constraints are enforced at a sufficiently large number of discrete times to ensure satisfaction of all constraints throughout the time period of interest. (Since the completion of this work, progress has been reported in ref. 10 on methods to track one or more most critical times and enforce constraints only at those times.) Analytical solutions are obtained for the temperature history and stresses in the structure. The mass minimizations are carried out by use of the general-purpose optimizer AESOP (ref. 11).

The analytical design procedure is applied to two studies: (1) A comparative structural efficiency study of several structural materials suitable for high-temperature structural applications - graphite/polyimide, graphite/epoxy, boron/aluminum, titanium, René 41, aluminum, carbon/carbon, and Lockalloy; and (2) a study of the effect of intensity and duration of heating on the required mass for these materials. Effects of certain simplifying assumptions made in the analysis are also assessed for selected final designs. The purposes of this paper are to describe the analytical design procedure and to present the results of the studies carried out with the procedure.

SYMBOLS

The values are given in both SI and U.S. Customary Units. The calculations were made in U.S. Customary Units.

c heat capacity, J/kg-^{o}C (Btu/lbm-^{o}F)

c_1, c_2 heat capacity of insulation and structural material, respectively, J/kg-^{o}C (Btu/lbm-^{o}F)

E_1, E_2 Young's modulus in fiber and transverse directions, respectively, Pa (lbf/in^2)

F	Tsai-Wu failure criterion
F_1	$= 1/X_T + 1/X_C$
F_2	$= 1/Y_T + 1/Y_C$
F_{11}	$= -1/X_T X_C$
F_{22}	$= -1/Y_T Y_C$
F_{66}	$= 1/S^2$
G	shear modulus, Pa (lbf/in^2)
g	constraint
k	thermal conductivity, W/m-^{o}C (Btu/in-sec-^{o}F)
k_1, k_2	thermal conductivity of insulation and structural material, respectively, W/m-^{o}C (Btu/in-sec-^{o}F)
NLAYER	number of layers in laminate
NTIMES	number of discrete times
N_x, N_y, N_{xy}	stress resultants, kN/m (lbf/in.)
N_{tx}, N_{ty}	thermal forces, kN/m (lbf/in.)
RT	room temperature
S	shear strength, Pa (lbf/in^2)
T	temperature, K (^{o}F)
T_a	allowable temperature, K (^{o}F)
T_{eq}	outer surface temperature, K (^{o}F)
$T_{eqo}, T_{peak}, T_{eqf}, \tau_{peak}, \tau_f$	parameters of temperature pulse (fig. 2), K (^{o}F)
T^*	optimum operating temperature, K (^{o}F) (fig. 3)
t_0, t_{45}, t_{90}	thickness of 0^o, ±45^o, and 90^o plies, respectively, cm (in.)
t_1, t_2	insulation and structure thicknesses, respectively, cm (in.)
V	Von Mises' stress criterion, Pa (lbf/in^2)
W	mass, kg (lbm)

X_T, X_C tensile and compressive strengths in fiber direction, respectively, Pa (lbf/in^2)

Y_T, Y_C tensile and compressive strengths in transverse direction, respectively, Pa (lbf/in^2)

x, y laminate coordinate directions

z_1, z_2 coordinates through depth of insulation and structure, respectively, cm (in.)

α_1, α_2 coefficients of thermal expansion in fiber and transverse directions, respectively, $^oC^{-1}$ ($^oF^{-1}$)

β edge-fixity coefficient

θ ply angle, deg

ν_1, ν_2 Poisson's ratio for fiber and transverse directions, respectively

ρ mass density, kg/m^3 (lbm/in^3)

ρ_1, ρ_2 mass density of insulation and structural materials, respectively, kg/m^3 (lbm/in^3)

σ_a allowable stress, Pa (lbf/in^2)

$\sigma_1, \sigma_2, \sigma_{12}$ stress components in laminar coordinate system, Pa (lbf/in^2)

τ time, sec

$\bar{\tau}$ period of time that constraints are imposed; monitoring time, sec

CONFIGURATION AND LOADS

The configuration, as shown in figure 1, consists of a layer of insulation attached to a structural layer. This configuration is assumed to be a localized region of a larger structure and is sufficiently small so that neither the mechanical loads nor the temperature vary significantly over the region. Also the region is assumed to be sufficiently far removed from restrained boundaries so that edge effects are negligible. The structural layer is subjected to a general set of inplane mechanical loads given by the stress resultants N_x, N_y, and N_{xy}, which are assumed to be time independent. The structural layer is either a filamentary composite laminate or a metal layer. No mechanical loads are applied to the insulation layer. The outer surface of the insulation is subjected to time-dependent heating, which is characterized by a temperature $T_{eq}(\tau)$. In the present work, the particular form of $T_{eq}(\tau)$ is the curve shown in figure 2. The shape of the curve (generally a third-order function of time for $\tau \leqq \tau_f$ and constant thereafter) is determined by the quantities T_{eqo}, T_{peak}, τ_{peak}, τ_f, and T_{eqf}.

ANALYTICAL DESIGN PROCEDURE

Thermal and Structural Analysis

Analysis of the temperature history is based on one-dimensional heat transfer through the depth of the insulation-structure configuration. The outer surface of the insulation has a prescribed temperature, and the back face of the structural layer is assumed to be an adiabatic surface. The temperature history throughout the insulation and structure is obtained by an analytical solution described in appendix A. The assumption that the back face of the structural layer is an adiabatic surface is known to be conservative. Quantification of the effects of the adiabatic assumption is described in appendix B, where this assumption is relaxed by permitting radiation from the back face of the structural layer, and temperatures for radiative and adiabatic back-face conditions are compared.

The structural analysis is based on calculating stresses and strains at a point in the structure resulting from a set of applied forces N_x, N_y, and N_{xy} and the temperature at that point. This approach neglects edge-boundary effects, especially those due to thermal stresses arising from restraint of thermal expansion; however, thermal stresses due to interlayer thermal property mismatch are included. The applied forces are assumed to be constant (i.e., time independent). The structural analysis based on these assumptions is described in appendix A. Effects of neglecting restrained thermal expansion due to edge restraint and effects of time-dependent loading are evaluated in appendix B. In the analysis, linear representations of the temperature dependence of the mechanical properties are used. In principle, any known variation of mechanical property with temperature may be input.

Design Objective and Constraints

The objective of the present procedure is to determine the insulation thickness t_1 and structural thickness t_2 for the configuration in figure 1 such that the total mass is a minimum and the structural temperature and stresses do not exceed prescribed allowable values throughout a span of time $\bar{\tau}$. The mass is given by

$$W = \rho_1 t_1 + \rho_2 t_2 \tag{1}$$

where for a composite laminate with 0°, $\pm 45^\circ$, and 90° plies

$$t_2 = t_0 + t_{45} + t_{90} \tag{2}$$

and for a metal structure t_2 is the metal thickness. The temperature constraint is

$$T(\tau) \leqq T_a \qquad (0 \leqq \tau \leqq \bar{\tau}) \qquad (3)$$

where T is the temperature of the structural layer and T_a is the allowable temperature of the structural layer. The value assigned to T_a is somewhat arbitrary and represents the maximum service temperature of the material for structural applications. In the case of filamentary composites, values of T_a are generally dictated by the integrity of the resin material. In this paper, values of T_a are based on current usage of the various materials in high-temperature applications and recommended temperature ranges from the appropriate literature (refs. 12 to 15).

The stress constraint for each layer of a filamentary composite laminate is expressed by a modified form of the Tsai-Wu failure criterion (ref. 16)

$$F = F_1\sigma_1 + F_2\sigma_2 + F_{11}\sigma_1^2 + F_{22}\sigma_2^2 + F_{66}\sigma_{12}^2 \leqq 1 \qquad (0 \leqq \tau \leqq \bar{\tau}) \qquad (4)$$

The coefficients F_1, F_2, F_{11}, F_{22}, and F_{66} in equation (4) are functions of the allowable stresses for the composite system and are all temperature dependent. The stress constraint for a metal layer is given by

$$F = V/\sigma_a \leqq 1 \qquad (0 \leqq \tau \leqq \bar{\tau}) \qquad (5)$$

where the Von Mises' stress criterion is

$$V = \left(\sigma_1^2 + \sigma_2^2 - \sigma_1\sigma_2 + 3\sigma_{12}^2\right)^{1/2} \qquad (6)$$

Before describing the analytical design procedure, it is instructive to describe the trade-off involved in designing an insulated structure. As shown in figure 3, the required mass of the load-carrying structure increases with operating temperature of the structure, primarily because of degradation of mechanical properties. The required mass of the insulation decreases with increasing operating temperature level. The total mass therefore attains a minimum for some temperature T^*. This optimum temperature may be significantly less than the allowable temperature indicated by T_a. It is shown subsequently that the difference between T^* and T_a is principally a function of the mechanical load.

Design Formulation

The design problem is formulated and solved as a nonlinear mathematical programming problem. The objective function is given by equation (1). The design variables consist of t_1 and either the set t_0, t_{45}, and t_{90} or t_2. The constraints are expressed by equation (3) and either equation (4) or (5). For convenience and in preparation for the discretization of the time

dependence of the constraints, equations (3) to (5) are written as nondimensional constraint functions

$$g_1(\tau) = T(\tau)/T_a - 1 \leqq 0 \qquad (0 \leqq \tau \leqq \bar{\tau}) \tag{7}$$

$$g_{j+1}(\tau) = F_j(\tau) - 1 \qquad (0 \leqq \tau \leqq \bar{\tau};\ j = 1, 2, \ldots \text{NLAYER}) \tag{8}$$

where F is given by equation (4) or (5). In addition to the behavior constraints in equations (7) and (8), minimum gage constraints are applied to the design variables.

Treatment of Constraints on Time-Dependent Quantities

In developing the present analytical design procedure, special attention was focused on the satisfaction of constraints on time-dependent temperatures and stresses (eqs. (7) and (8)). Some guidance was available from reference 9, which treated the optimum design of an ablating heat shield. In reference 9 the constraints on time-dependent quantities were replaced by time-integrated averages of the original constraints. The representations were carefully formulated to exclude violations at any point in time but, as pointed out in reference 9, had the disadvantage that temperatures and stresses were somewhat insensitive to structural size parameters because of the smoothing effect of the integral representation of the constraints. Early in the present work, alternative approaches were considered, including other integral representations (ref. 17) and ideas for tracking one or more most critical times and enforcing constraints only at those times. The approach decided upon was a simple time slicing, whereby constraints were enforced at a sufficiently large number of discrete times in the time period of interest. A schematic representation of the discrete-times approach for temperature constraints is shown in figure 4.

In the discrete-times approach, the constraints of equations (7) and (8) are replaced by

$$g_i = T(\tau_i)/T_a - 1 \leqq 0 \qquad (i = 1, \text{NTIMES}) \tag{9}$$

$$g_{\text{NTIMES}+i\cdot j} = F_j(\tau_i) - 1 \leqq 0$$

$$(i = 1, \text{NTIMES};\ j = 1, 2, \ldots \text{NLAYER}) \tag{10}$$

Thus the total number of constraints is

$$(1 + \text{NLAYER})(\text{NTIMES})$$

Because the number of constraints is proportional to the number of discrete times NTIMES, it is of interest to determine how large NTIMES must be for typical calculations. The answer is problem dependent, but studies carried out and documented in reference 4 and in a subsequent section of this paper indicate that, for the types of insulated structures under the types of heating histories considered herein, only a few (three or four) discrete times are needed.

Sizing Technique

The computer program used to perform the optimizations is a general-purpose optimizer denoted AESOP (ref. 11), which accounts for constraints using an exterior penalty function approach (ref. 17). The AESOP code contains several optimization algorithms that can be selected in various combinations by the user. The approach used here was a combination of adaptive search and pattern search. These algorithms are described in reference 11.

APPLICATIONS AND DISCUSSION

Overview

In this section the design procedure is used to carry out design studies. First a preliminary study is performed to assess the minimum number of discrete times needed to obtain minimum-mass designs. Next the design procedure is applied to an efficiency study for eight structural materials over a wide range of loads and two heating conditions representative of high-speed flight of winged reentry vehicles (refs. 18 and 19). The materials in the study include graphite/epoxy, graphite/polyimide, boron/aluminum, aluminum, titanium, René 41, carbon/carbon, and Lockalloy. A study is then carried out to assess the effect on minimum mass of heating duration and intensity for the eight materials. Finally results are presented to assess the effects of certain simplifying assumptions made in the analysis.

Materials Used In Studies

The eight structural materials selected for the studies are listed in table I along with averaged values used for thermal conductivity, specific heat capacity, and density, as well as the allowable temperatures used in the studies. Properties are also given for the insulation which is LI-900 reusable surface insulation. Mechanical properties for the structural materials were obtained from references 4 and 12 to 15 and are listed in table II. Minimum gages considered are given in table III.

Discrete-Times Convergence Study

The purpose of this section is to show approximately how many discrete times are needed for a typical design problem.

The study is carried out for a Gr/E panel with an outer surface temperature history (fig. 2) characterized by T_{peak} = 1089 K (1500° F), τ_{peak} = 700 sec, τ_f = 1500 sec, and T_{eqf} = 297 K (75° F) and loads of $N_x = N_y = -700$ kN/m (-4000 lbf/in.) and N_{xy} = 525 kN/m (3000 lbf/in.). The monitoring time $\bar{\tau}$ was 6000 sec. Designs were obtained for 3 to 15 time slices. Final mass is plotted against the number of slices in figure 5. The plot indicates that only three or four discrete times are necessary to give satisfactory results in the sense that increasing the number of discrete times does not improve the result. Figure 6(a) shows the temperature and stress response (in the 45° ply) in the final design. The response of temperature is most important to this design (i.e., only the temperature constraint is critical for $\tau > 0$). Observe that the temperature response is a smooth curve with a single local maximum. Thus only a small number of equally spaced time slices are needed to define properly the critical temperature. If a more severe or complicated heating pulse is applied, the temperature response would still be smooth and gradual. This assertion is based on previous analyses (refs. 4 and 20) and occurs because the insulation has a smoothing (dampinglike) effect on the thermal response of the structure.

The stress-response curve is somewhat more complicated than the temperature response but again only has a single local maximum. Since stress is not critical for $\tau > 0$, it is not clear from this example what effect the stress response has on the number of discrete times required. To investigate this effect, consider the Gr/E panel with higher loads of $N_x = N_y = -1.05$ MN/m (-6000 lbf/in.) and N_{xy} = 700 kN/m (4000 lbf/in.), in which stresses are critical for $\tau > 0$ (fig. 6(b)). The plot of final mass against the number of time slices is shown in figure 7 and indicates that, despite the criticality of stress, only three or four time slices are needed for a satisfactory answer.

Thermal-Structural Efficiency Study

This study is a comparative evaluation of the performance of the eight materials over a wide spectrum of load levels for two heating conditions. Except for René 41 and carbon/carbon, each material is protected by a layer of insulation. The first (low) heating condition is characterized by T_{peak} = 1089 K (1500° F), and the second (high) heating condition has a value of T_{peak} = 1533 K (2300° F). In both cases τ_{peak} = 700 sec and τ_f = 2000 sec. In all calculations $N_y = N_x$ and $N_{xy} = (2/3)N_x$. The results for the low-heating condition are presented in figure 8. At high-load levels Gr/PI gives the lowest mass, followed by B/Al. Neither René 41 nor carbon/carbon are competitive at high-load levels. For N_x between 175 and 525 kN/m (1000 and 3000 lbf/in.) René 41 (uninsulated) and Lockalloy give the lowest mass, and for N_x less than 175 kN/m (1000 lbf/in.) carbon/carbon gives the lowest mass. These results suggest possible benefits of these unprotected materials for lightly loaded regions, such as control surfaces. The curves for Lockalloy and aluminum have a corner or discontinuity that represents a change in the character of the final design - designs to the left of the corner are operating at the allowable temperature and allowable stress, whereas designs to the right of the corner are operating at the allowable stress but with temperatures less than the allowable value.

For the high-heating case in which T_{peak} = 1533 K (2300° F) (fig. 9), Gr/PI again gives the lowest mass for the highest load values (above about 1.05 MN/m (6000 lbf/in.)). For loads between 700 kN/m and 1.05 MN/m (4000 and 6000 lbf/in.), B/Al designs have the lowest mass. Lockalloy gives the lowest mass designs for N_x between 262 and 700 kN/m (1500 and 4000 lbf/in.), and carbon/carbon gives the lowest mass for loads less than 262 kN/m (1500 lbf/in.). Based on these results uninsulated carbon/carbon and insulated Lockalloy again seem to have significant potential for application to lightly loaded regions, and for more highly loaded regions such as the wing, insulated Gr/PI, B/Al, Gr/E, and titanium seem to be worthy of consideration. These results are based on a simplified model and consider only strength and temperature requirements.

Characteristics of Final Designs

The main characteristics of selected designs in figures 8 and 9 are summarized in tables IV(a) to IV(l). Tables IV(a) to IV(f) have results for the lower heating case where T_{peak} = 1089 K (1500° F) for values of N_x from 0 to -2.63 MN/m (-15 000 lbf/in.) in increments of 525 kN/m (3000 lbf/in.). Tables IV(g) to IV(l) have corresponding results for the higher heating case where T_{peak} = 1533 K (2300° F). The tables contain for each material the final mass, maximum temperature response in the final design and the time it occurs, and maximum stress ratio and the time it occurs. The tabulations are presented to provide check results for other investigators and to show some features of the designs. For the lowest loads, the structures operate at their allowable temperatures and the design problem is one of providing minimum-mass designs for temperature requirements. As higher loads are considered, strength constraints become important and a trade-off mechanism becomes operative, whereby high-temperature operation with less insulation, lower allowable stress, and a heavier structure is balanced against lower temperature operation with more insulation, higher allowable stress, and a lighter structure. For each insulated material, a load value is eventually reached where the trade-off favors lower temperature operation to maintain a sufficiently high allowable stress. As suggested by figure 3, the structural temperature in such designs is below the allowable temperature of the material and the designs are governed primarily by strength constraints.

In some cases, the temperature in the final design is well below the allowable temperature. For example, Lockalloy under a load of N_x = -2.63 MN/m (-15 000 lbf/in.) and T_{peak} = 1533 K (2300° F) attains a maximum temperature which is only 49 percent of its allowable temperature. This effect points out that contrary to conventional design practice, the minimum-mass insulated heat-sink structure is not necessarily one in which the structure operates at its allowable temperature. This observation was previously made for an ablation panel in reference 9. To bring out the significance of this observation, consider a set of Lockalloy designs for T = 1533 K (2300° F) at the load range of 0 to -2.63 MN/m (-15 000 lbf/in.), as described in table IV. A set of corresponding designs, based on the conventional practice of assuming operation at the allowable temperature, is generated for comparison. The latter designs are obtained by first sizing the structural thickness from the applied mechanical loads and the allowable stress at 700 K (800° F), then fixing the structural

thickness, and then carrying out design calculations to size the insulation thickness required to maintain this temperature. Design masses from this conventional procedure and the present method are compared in figure 10. Since the structure has a peak temperature response at or close to the allowable temperature, there is little difference between the designs at loads below about 525 kN/m (3000 lbf/in.). Significant differences occur at higher loads. For example, at 2.10 MN/m (12 000 lbf/in.) the conventional design has 40 percent more mass than the present design, and at 2.63 MN/m (15 000 lbf/in.) the conventional design has 47 percent more mass. These results suggest that design of structures for thermal applications should be based on simultaneous consideration of temperature and structural requirements.

Effect of Heating Duration and Intensity

This section describes a study of the effects of duration and intensity of heating on minimum mass. Designs are obtained corresponding to high and low values of intensity and duration of heating associated with winged reentry vehicles (ref. 18), as described by the parameters T_{peak} and τ_f, respectively. Values used for τ_f were 1500 sec and 2000 sec, and values for T_{peak} were 1089 K (1500° F) and 1533 K (2300° F).

Results of the study are presented in table V. Both intensity and duration of heating have significant effects on the designs. For example, increasing τ_f for B/Al with T_{peak} = 1533 K (2300° F) led to an increase in required mass of 18 percent. Increasing both T_{peak} and τ_f for the same case led to a mass increase of 41 percent.

Effects of Simplifying Assumptions

This section summarizes the effects of certain assumptions made in the analysis; namely, neglect of edge effects due to restraint of thermal expansion, neglect of time dependence of the mechanical loads, and neglect of heat loss from the back face of the structural layer. Details are given in appendix B.

Restrained thermal expansion.- Calculations are carried out for Gr/E, titanium, and Lockalloy. Figure 11 shows a plot of design mass as a function of an edge-fixity coefficient β which varies between 0 and 1. A value of $\beta = 1$ corresponds to completely restrained expansion, and $\beta = 0$ corresponds to unrestrained expansion. Results indicate that the effects of restrained thermal expansion are negligibly small for Gr/E, are moderate for titanium (a 22-percent increase in design mass as β is increased from 0 to 1), and large for Lockalloy (an 83-percent increase as β is increased from 0 to 1).

Time-dependent loading.- To assess the effects of time dependence of the mechanical loads, design calculations are repeated for two selected cases: (1) Graphite/epoxy with a maximum load N_x = -1.05 MN/m (-6000 lbf/in.); and (2) titanium with a maximum load of -1.58 MN/m (-9000 lbf/in.). The mechanical loads varied with time according to figure 12, which is representative of load against time during reentry (ref. 21). Designs are compared with those based on constant loading. Results are given in table VI, which shows that time-

dependent loading has a very small effect on the final design mass. Observe however that in the designs for time-dependent loads, the maximum stress ratio occurred at the times of maximum load (1600 sec) for both materials rather than times of peak temperature (2800 sec for Gr/E and 2000 sec for titanium) when loads were constant. There was no appreciable effect on the temperature responses for either material as a result of time-dependent loads.

Heat transfer from back face of structure.- To assess the effect of neglecting heat transfer from the back face of the structural layer, thermal analyses of selected designs, which included radiative heat transfer from the back face, were carried out. A finite-element thermal model was formulated by using the SPAR thermal analyzer (ref. 22). In the SPAR model the back face of the structural layer was permitted to radiate to a medium at room temperature. Temperature histories were calculated for the eight final designs in table IV(d) with the adiabatic back face and the radiating back face. Table VII contains a comparison of the peak temperatures for the two conditions. The largest change in peak temperature is 33 percent for titanium. This significant temperature difference does not necessarily translate into a large effect on design mass. As an example, the increase in strength of titanium from 548 K to 451 K (527° F to 352° F) is about 16 percent. If the structural mass of the titanium design is assumed to be decreased by 16 percent while the insulation mass remains unchanged, the total required mass is decreased by about 11 percent.

CONCLUDING REMARKS

A procedure is described for obtaining minimum-mass designs of insulated composite or metal structural panels subjected to transient heating and mechanical loads. The procedure uses nonlinear mathematical programming techniques, and analytical solutions are used for temperature histories and stresses in the structure. An important aspect of the present problem is the need to enforce constraints on transient temperatures and stresses. In the present procedure, the constraints are enforced at a finite number of time slices or discrete times over the time period of interest, and satisfactory results are obtained with a small number of times.

To simplify the analysis, edge effects due to restrained thermal expansion are neglected, constant (time independent) mechanical loads are assumed, and heat loss from the back face of the structure is neglected. The errors in design mass introduced by these assumptions are examined. Neglecting edge effects can lead to sizable errors; neglecting heat loss from the back face has a smaller but significant effect; and time dependence of loading has a negligible effect on the designs.

The design procedure is used to perform structural efficiency studies for eight materials for two representative values of peak external heating and a range of mechanical load levels. Materials considered are graphite/polyimide, graphite/epoxy, boron/aluminum, titanium, aluminum, René 41, carbon/carbon, and Lockalloy. All except René 41 and carbon/carbon have a layer of reusable surface insulation. For the lower heating condition graphite/polyimide gave the lowest mass except at the lowest load levels, whereas René 41 and carbon/carbon gave the lowest mass. For the higher heating condition graphite/

polyimide again gave the lowest mass for high and moderate loads, whereas Lockalloy and carbon/carbon gave the lowest mass at low-load levels. Additional calculations indicate that intensity and duration of heating can have a substantial effect on design mass.

Examinations of the characteristics of the final designs indicate that for sufficiently high mechanical loads, the optimum structure has a temperature response substantially less than the recommended allowable temperature of the material. This result is contrary to the usual engineering practice of basing a design on the higher temperature operation. Comparisons of several Lockalloy designs obtained by the present procedure with those based on operation at higher temperatures indicate that significant mass savings may be attainable by lower temperature operation.

Langley Research Center
National Aeronautics and Space Administration
Hampton, VA 23665
October 11, 1979

APPENDIX A

THERMAL AND STRUCTURAL ANALYSIS

TEMPERATURE HISTORY

The solution for the temperature history is obtained by using the analysis of heat transfer in a two-layered configuration given in reference 23. The purpose of this appendix is to outline the approach used in reference 23 and specialize that general result for the present problem (fig. 1). The governing equations, boundary conditions, and initial conditions are

$$k_1 \frac{\partial^2 T_1}{\partial z_1^2} = \rho_1 c_1 \frac{\partial T_1}{\partial \tau} \tag{A1}$$

$$k_2 \frac{\partial^2 T_2}{\partial z_2^2} = \rho_2 c_2 \frac{\partial T_2}{\partial \tau} \tag{A2}$$

$$k_1 \left.\frac{\partial T_1}{\partial z_1}\right|_{z_1=0} = k_2 \left.\frac{\partial T_2}{\partial z_2}\right|_{z_2=t_2} \tag{A3}$$

$$T_1(0,\tau) = T_2(t_2,\tau) \tag{A4}$$

$$T_1(t_1,\tau) = T_{eq}(\tau) \tag{A5}$$

$$\left.\frac{\partial T_2}{\partial z_2}\right|_{z_2=0} = 0 \tag{A6}$$

$$T_1(z_1,0) = T_2(z_2,0) = T_0 \tag{A7}$$

Equations (A1) and (A2) govern the temperatures in the insulation and structural layers, respectively. Equations (A3) and (A4) define the continuity of heat flux and temperature at the insulation-structure interface. Equation (A5) is the specification of the temperature history at the upper surface of the insulation. Equation (A6) states that no heat is lost through the back face of the structural layer. Equation (A7) defines the initial conditions on temperatures. As pointed out in reference 8, the assumption that no heat is transferred from the back face of the structural layer is conservative, especially when radiation

from the back face to internal heat sinks represents a significant heat loss. In such cases, however, it would probably be necessary to insulate the back face of the structure to protect internal equipment from excessive heating by thermal radiation. Further discussion of the effects of this assumption is presented in appendix B. Solutions to the equations are obtained in reference 23. The expression for the average temperature in the structural layer is of interest for the current problem. This solution is

$$T(\tau) = T_{eq}(0) + \left[T_0 - T_{eq}(0)\right] \sum_{n=1}^{\infty} \frac{\sin \gamma_n}{\gamma_n H_n} e^{-\gamma_n^2 p}$$

$$+ \int_0^p \left[1 - \sum_{n=1}^{\infty} \frac{\sin \gamma_n}{\gamma_n H_n} e^{-\gamma_n^2 (p-u)}\right] \frac{dT_{eq}(u)}{du} du \tag{A8}$$

where γ_n is the nth root of

$$\beta\xi \tan \gamma \tan \frac{\gamma}{\beta} = 1 \tag{A9}$$

$$\beta = \frac{k_1 c_2 \rho_2 t_2}{k_2 c_1 \rho_1 t_1} \tag{A10}$$

$$\xi = \frac{k_2 t_1}{k_1 t_2} \tag{A11}$$

$$H_n = \frac{\gamma_n}{2}\left[\left(\beta\xi + \frac{1}{\beta}\right) \cos \gamma_n \sin \frac{\gamma_n}{\beta} + (1 + \xi) \sin \gamma_n \cos \frac{\gamma_n}{\beta}\right] \tag{A12}$$

and dimensionless time is

$$p = \frac{k_2}{c_2 \rho_2 t_2^2} \tau \tag{A13}$$

APPENDIX A

In the present work the outer surface temperature $T_{eq}(\tau)$ is represented as (see fig. 2)

$$T_{eq}(\tau) = a_{eq} + b_{eq}\tau + c_{eq}\tau^2 + d_{eq}\tau^3 \qquad (\tau \leq \tau_f) \qquad (A14)$$

$$T_{eq}(\tau) = T_{eqf} \qquad (\tau > \tau_f) \qquad (A15)$$

The coefficients in equation (A14) are expressed in terms of the parameters of the curve in figure 2. The conditions for evaluating the coefficients are that the curve of equation (A14) passes through the three points noted on the curve and has a zero slope at $\tau = \tau_{peak}$. The results are

$$d_{eq} = \frac{T_{eqf} - T_{eqo} + (T_{peak} - T_{eqo})\left[\left(\frac{\tau_f}{\tau_{peak}}\right)^2 - 2\frac{\tau_f}{\tau_{peak}}\right]}{\tau_f(\tau_{peak} - \tau_f)^2}$$

$$c_{eq} = \frac{T_{eqo} - T_{peak}}{\tau_{peak}^2} - 2\tau_{peak}d_{eq}$$

$$b_{eq} = -2\tau_{peak}c_{eq} - 3\tau_{peak}^2 d_{eq}$$

$$a_{eq} = T_{eqo}$$

The coefficients b_{eq}, c_{eq}, and d_{eq} are nondimensionalized by defining

$$\beta_{eq} = b_{eq}/R$$

$$\gamma_{eq} = c_{eq}/R^2$$

$$\delta_{eq} = eq/R^3$$

where

$$R = \frac{k_2}{c_2\rho_2 t_2^2}$$

Substituting equations (A14) and (A15) into equation (A8) gives the following solutions:

APPENDIX A

$$T = T_{eq}(0) + \beta_{eq}p + \gamma_{eq}p^2 + \delta_{eq}p^3 + \left[T_0 - T_{eq}(0)\right] \sum_{n=1}^{\infty} \frac{\sin \gamma_n}{\gamma_n H_n} e^{-\gamma_n^2 p}$$

$$- \sum_{n=1}^{\infty} \frac{\sin \gamma_n}{\gamma_n H_n} \left\{ \frac{\beta_{eq}}{\gamma_n^2} \left(1 - e^{\gamma_n^2 p}\right) + \frac{2\gamma_{eq}}{\gamma_n^4} \left(e^{-\gamma_n^2 p} + \gamma_n^2 p - 1\right) \right.$$

$$\left. + 3\delta_{eq} \left[\frac{p^2}{\gamma_n^2} - \frac{2p}{\gamma_n^4} + \frac{2}{\gamma_n^6} \left(1 - e^{-\gamma_n^2 p}\right) \right] \right\} \qquad (\tau \leq \tau_f) \qquad \text{(A16)}$$

$$T = T_{eqf} + \left[T_0 - T_{eq}(0)\right] \sum_{n=1}^{\infty} \frac{\sin \gamma_n}{\gamma_n H_n} e^{-\gamma_n^2 p_f}$$

$$- \sum_{n=1}^{\infty} \frac{\sin \gamma_n}{\gamma_n H_n} \left(\frac{\beta_{eq}}{\gamma_n^2} \left[e^{\gamma_n^2 (p_f - p)} - e^{\gamma_n^2 p} \right] \right.$$

$$+ \frac{2\gamma_{eq}}{\gamma_n^4} \left[e^{-\gamma_n^2 p} - e^{\gamma_n^2 (p_f - p)} \left(1 - \gamma_n^2 p_f\right) \right]$$

$$+ 3\delta_{eq} \left\{ \frac{p_f^2}{\gamma_n^2} e^{\gamma_n^2 (p_f - p)} - \frac{2p_f}{\gamma_n^4} e^{\gamma_n^2 (p_f - p)} \right.$$

$$\left. \left. + \frac{2}{\gamma_n^6} \left[e^{\gamma_n^2 (p_f - p)} - e^{-\gamma_n^2 p} \right] \right\} \right) \qquad (\tau > \tau_f) \qquad \text{(A17)}$$

where

$$p_f = \frac{k_2}{c_2 \rho_2 t_2^2} \tau_f$$

In the evaluation of equations (A16) and (A17), six terms of the series have provided sufficiently accurate temperatures. In the general case where both t_1

and t_2 are nonzero, the roots of equation (A9) are extracted numerically by a systematic search. For the special case where $t_1 = 0$, that is, the insulation layer is omitted, the roots of equation (A9) are given by

$$\gamma_n = \left(n - \frac{1}{2}\right)\pi \tag{A18}$$

and for this case equation (A12) reduces to

$$H_n = \left(n - \frac{1}{2}\right)\frac{\pi}{2}(-1)^{n-1} \tag{A19}$$

STRESS ANALYSIS

The stresses in the laminate are computed from elementary thermoelastic lamination theory (ref. 24). The constitutive equations for a balanced symmetric laminate under inplane mechanical and thermal loading are written

$$\begin{Bmatrix} N_x + N_{tx} \\ N_y + N_{ty} \\ N_{xy} \end{Bmatrix} = \begin{bmatrix} A_{11} & A_{12} & 0 \\ A_{12} & A_{22} & 0 \\ 0 & 0 & A_{66} \end{bmatrix} \begin{Bmatrix} e_x \\ e_y \\ e_{xy} \end{Bmatrix} \tag{A20}$$

where N_x, N_y, and N_{xy} are constant (i.e., time independent) applied mechanical forces per unit width of the laminate and A_{11}, A_{12}, A_{22}, and A_{66} are laminate stiffnesses, given by

$$A_{11} = \sum_{i=1}^{NLAYER} \bar{Q}_{11} t_i \tag{A21a}$$

$$A_{12} = \sum_{i=1}^{NLAYER} \bar{Q}_{12} t_i \tag{A21b}$$

$$A_{22} = \sum_{i=1}^{NLAYER} \bar{Q}_{22} t_i \tag{A21c}$$

$$A_{66} = \sum_{i=1}^{NLAYER} \bar{Q}_{66} t_i \tag{A21d}$$

where t_i is the thickness of the ith layer. The thermal forces N_{tx} and N_{ty} are given by

$$N_{tx} = \sum_{i=1}^{NLAYER} \left[(\bar{Q}_{11}\alpha_x + \bar{Q}_{12}\alpha_y + \bar{Q}_{16}\alpha_{xy})t\right]_i (T - T_{ref}) \tag{A22}$$

$$N_{ty} = \sum_{i=1}^{NLAYER} \left[(\bar{Q}_{12}\alpha_x + \bar{Q}_{22}\alpha_y + \bar{Q}_{26}\alpha_{xy})t\right]_i (T - T_{ref}) \tag{A23}$$

where T_{ref} is the stress-free temperature and

$$\left.\begin{aligned} \alpha_x &= m^2\alpha_1 + n^2\alpha_2 \\ \alpha_y &= n^2\alpha_1 + m^2\alpha_2 \\ \alpha_{xy} &= 2mn(\alpha_1 - \alpha_2) \end{aligned}\right\} \tag{A24}$$

In these equations, $m = \cos\theta$, $n = \sin\theta$, θ is the lamina ply angle, and

$$\bar{Q}_{11} = Q_{11}m^4 + 2(Q_{12} + 2Q_{66})n^2m^2 + Q_{22}n^4 \tag{A25a}$$

$$\bar{Q}_{22} = Q_{11}n^4 + 2(Q_{12} + 2Q_{66})n^2m^2 + Q_{22}m^4 \tag{A25b}$$

$$\bar{Q}_{12} = (Q_{11} + Q_{22} - 4Q_{66})n^2m^2 + Q_{12}(n^4 + m^4) \tag{A25c}$$

$$\bar{Q}_{16} = (Q_{11} - Q_{12} - 2Q_{66})nm^3 + (Q_{12} - Q_{22} + 2Q_{66})n^3m \tag{A25d}$$

$$\bar{Q}_{26} = (Q_{11} - Q_{12} - 2Q_{66})n^3m + (Q_{12} - Q_{22} + 2Q_{66})nm^3 \tag{A25e}$$

$$\bar{Q}_{66} = (Q_{11} - Q_{22} - 2Q_{12} - 2Q_{66})m^2n^2 + Q_{66}(n^4 + m^4) \tag{A25f}$$

$$\left.\begin{aligned} Q_{11} &= \frac{E_1}{1 - \nu_1\nu_2} \\ Q_{22} &= \frac{E_2}{1 - \nu_1\nu_2} \\ Q_{66} &= G \\ Q_{12} &= \nu_1 Q_{22} \end{aligned}\right\} \tag{A26}$$

where E_1, E_2, ν_1, ν_2, and G are functions of temperature. The laminate strains e_x, e_y, and e_{xy} are obtained by solving equation (A20). The lamina strains are obtained as follows:

$$\left.\begin{aligned} e_1 &= m^2e_x + n^2e_y + mne_{xy} \\ e_2 &= n^2e_x + m^2e_y - mne_{xy} \\ e_{12} &= 2mn(e_y - e_x) + (m^2 - n^2)e_{xy} \end{aligned}\right\} \tag{A27}$$

and the stresses in each lamina are given by

$$\left.\begin{aligned} \sigma_1 &= Q_{11}e_1 + Q_{12}e_2 - (Q_{11}\alpha_1 + Q_{12}\alpha_2)(T - T_{ref}) \\ \sigma_2 &= Q_{12}e_1 + Q_{22}e_2 - (Q_{12}\alpha_1 + Q_{22}\alpha_2)(T - T_{ref}) \\ \sigma_{12} &= Q_{66}e_{12} \end{aligned}\right\} \tag{A28}$$

The stresses in equations (A28) neglect edge effects, particularly effects of restrained thermal expansion due to edge supports. Estimates of the importance of such thermal stresses are considered in appendix B.

APPENDIX B

EFFECTS OF RESTRAINED THERMAL EXPANSION, TIME-DEPENDENT LOADS, AND BACK-FACE THERMAL BOUNDARY CONDITION

The purpose of this appendix is to quantify effects of certain simplifications employed in the analysis. These simplifications include neglect of edge effects due to restrained thermal expansion, neglect of time variations of the applied mechanical loads, and neglect of heat loss from the back face of the structural layer.

RESTRAINED THERMAL EXPANSION

The stress analysis used in the design procedure and described in appendix A is based on stresses and strains at a point and thus does not incorporate edge effects, particularly effects of thermal stresses due to restraint of thermal expansion by edge fixity. The following analysis is an attempt to account, in an approximate manner, for the effects on design mass of thermal stresses due to edge fixity. If the temperature of a panel is raised while thermal expansion is prevented, the panel develops forces given by

$$\left.\begin{aligned} N_x &= -N_{tx} \\ N_y &= -N_{ty} \\ N_{xy} &= 0 \end{aligned}\right\} \tag{B1}$$

when N_{tx} and N_{ty} are thermal forces defined in appendix A. For the special case of an isotropic layer

$$N_x = N_y = -\frac{E\alpha h}{1 - \nu}(T - T_{ref}) \tag{B2}$$

where E is Young's modulus, α is the coefficient of thermal expansion, ν is Poisson's ratio, and h is the thickness of the layer. Equations (B1) correspond to complete restraint of inplane displacement. For completely unrestrained expansion, the forces N_x and N_y are zero. This circumstance suggests the introduction of an edge-fixity coefficient β, in which thermal stresses due to edge restraint are given by

$$\left.\begin{aligned} N_x &= -\beta N_{tx} \\ N_y &= -\beta N_{ty} \end{aligned}\right\} \tag{B3}$$

where

$$0 \leq \beta \leq 1$$

Completely fixed edges correspond to $\beta = 1$, and free edges correspond to $\beta = 0$. The analysis in appendix A is modified to incorporate equations (B3) by replacing N_{tx} by $(1 - \beta)N_{tx}$ and N_{ty} by $(1 - \beta)N_{ty}$ in equation (A20).

Evaluation of thermal-stress effects is carried out for three materials: Lockalloy, titanium, and graphite/epoxy. These materials were chosen because their properties result in high, intermediate, and low values of N_{tx} and N_{ty}. (See app. A and eq. (B2).) The results are shown in figure 11, wherein the optimum mass for the three materials is plotted as a function of β. Designs correspond to $N_x = -1.58$ MN/m (-9000 lbf/in.), $T_{peak} = 1089$ K (1500° F), and $\tau_f = 2000$ sec. The designs for $\beta = 0$ are listed in table IV(d). Figure 11 indicates that thermal stress due to edge fixity may have a significant effect on mass. This effect is apparent for Lockalloy, wherein the mass corresponding to $\beta = 1$ is 83 percent higher than the mass when $\beta = 0$. The change for titanium is 22 percent and essentially zero for graphite/epoxy. The importance of the thermal stress term is situational dependent. These results suggest the need to extend the design procedure to finite panels, wherein edge effects would naturally be included. Another benefit from extending the current procedure to finite panels is to enable buckling requirements to be properly included in the design of insulated panels.

TIME-DEPENDENT LOADING

Design calculations presented and discussed in the main text are based on constant applied mechanical loads. In an actual application, such as reentry, the loads vary with time. This section describes calculations to examine designs of time dependence of the loads. Figure 12 depicts a representative plot of amplitude of force (load factor) against time during reentry (ref. 21). As indicated in figure 12, all three load components are assumed to have the same time variation.

Calculations are carried out for two selected designs: Graphite/epoxy with a maximum load of $N_x = -1.05$ MN/m (-6000 lbf/in.) and titanium with a maximum load of -1.58 MN/m (-9000 lbf/in.). Results given in table VI show that time-dependent loading has a very small effect on the final design mass. In the designs for time-dependent loads, the maximum stress ratio occurred at the times of maximum load (1600 sec) for both materials rather than at the times of peak temperature (2800 sec for Gr/E and 2000 sec for titanium) when loads were constant. There was no appreciable effect on the temperature responses for either material as a result of time-dependent loads.

BACK-FACE THERMAL BOUNDARY CONDITION

As stated in the main text, the analysis of the temperature history given in appendix A incorporates the assumption that no heat flow takes place from

the back face of the structural layer. This assumption follows the precedents set by previous analyses of similar configurations and leads to conservative calculated temperatures. The purpose of this section is to provide some quantification of the effects of that assumption.

In order to carry out this quantification, a finite-element thermal model was formulated by using the SPAR thermal analyzer (ref. 22). In the SPAR model, the back face of the structural layer was permitted to radiate to a medium at room temperature. Temperature histories were calculated for the eight final designs from table IV(d). Table VII contains a comparison of the peak temperatures for the adiabatic and radiating boundary conditions. The largest change in peak temperature is 33 percent for titanium, and the smallest change is for René 41 and carbon/carbon. The effect of radiation might have been expected to be largest for the higher temperature materials. Certainly more heat is transferred from the back face of the high-temperature materials than the low-temperature materials. However the difference in temperatures from analyses with and without back-face radiation is not necessarily greater for the high-temperature materials. Other considerations are involved and the following explanation is offered. Inspection of the thermal properties and the response for the eight materials indicate an inverse correlation between the heat-storage term $\rho_2 c_2 t_2 \frac{dT_2}{d\tau}$ and the difference in temperatures in the two columns of table VII. From elementary energy conservation, a high value of heat storage leads to a high rate of radiation heat transfer from the back face of the structure. This result in turn requires a high, structural wall temperature. Conversely, the materials with low-heat storage (notably titanium and B/Al) tend to have lower wall temperatures. The temperatures in the left column of table VII are upper bounds to the corresponding temperatures in the right column. When radiation is included, the higher storage materials have structural temperatures closer to the adiabatic values than the low-storage materials, and hence the effect of the back wall radiation is greatest for these low-storage materials.

Although the effect of the back-face boundary conditions has a fairly sizable effect on some peak temperatures, it does not necessarily have a large effect on design mass. As an example, consider the largest difference in temperature being that of titanium. The increase in allowable stress of titanium from 548 K to 451 K (527° F to 352° F) is about 16 percent. If the structural mass of the titanium design is assumed to be decreased by 16 percent and the insulation mass remains unchanged, the total required mass is decreased by about 11 percent.

REFERENCES

1. Dexter, H. Benson; and Davis, John G., Jr., eds.: Graphite/Polyimide Composites. NASA CP-2079, 1979.

2. Adelman, Howard M.; and Robinson, James C.: Recent Advances in Thermal-Structural Analysis and Design. NASA CP-2065, 1978, pp. 897-941.

3. Thornton, Earl A.; and Wieting, Allan R.: Recent Advances in Thermostructural Finite Element Analysis. NASA CP-2065, 1978, pp. 851-896.

4. Adelman, Howard M.; Sawyer, Patricia L.; and Shore, Charles P.: Optimum Design of Structures at Elevated Temperatures. AIAA J., vol. 17, no. 6, June 1979, pp. 622-629.

5. Davidson, John R.: Optimum Design of Insulated Tension Members Subjected to Aerodynamic Heating. NASA TN D-117, 1959.

6. Davidson, John R.; and Dalby, James F.: Optimum Design of Insulated Compression Plates Subjected to Aerodynamic Heating. NASA TN D-520, 1961.

7. Harris, Robert S., Jr.; and Davidson, John R.: Methods for Determining the Optimum Design of Structures Protected From Aerodynamic Heating and Application to Typical Boost-Glide or Reentry Flight Paths. NASA TN D-990, 1962.

8. Rivello, Robert M.: Preliminary Design Methods for the Optimization of Insulated Structures for Hypersonic Cruise Vehicles. Rep. No. CF-3085 (Contract NOw 62-0604-c), Appl. Phys. Lab., Johns Hopkins Univ., May 15, 1964. (Available from DDC as AD 465 784.)

9. Thornton, William A.; and Schmit, Lucien A., Jr.: The Structural Synthesis of an Ablating Thermostructural Panel. NASA CR-1215, 1968.

10. Haftka, Raphael T.; and Shore, Charles P.: Approximation Methods for Combined Thermal/Structural Design. NASA TP-1428, 1979.

11. Jones, R. T.; and Hague, D. S.: Application of Multivariable Search Techniques to Structural Design Optimization. NASA CR-2038, 1972.

12. Hofer, K. E., Jr.; Rao, N.; and Larsen, D.: Development of Engineering Data on the Mechanical and Physical Properties of Advanced Composites Materials. AFML-TR-72-205-PT-2, U.S. Air Force, Feb. 1974. (Available from DDC as AD A01 5907.)

13. Metallic Materials and Elements for Aerospace Vehicle Structures - Volume 2. MIL-HDBK-5C, U.S. Dep. Def., Sept. 15, 1976.

14. White, D. M.: Development of a Thermal Protection System for the Wing of a Space Shuttle Vehicle - Phase 2. NASA CR-148908, 1972.

15. Fenn, Raymond W., Jr.; Coons, W. C.; Crooks, Donald D.; Neiman, Alfred S.; Robinson, John; and Watts, Glenn H.: Evaluation of BE-38% Al Alloy. NASA CR-64343, 1965.

16. Narayanaswami, R.; and Adelman, Howard M.: Evaluation of the Tensor Polynomial and Hoffman Strength Theories for Composite Materials. J. Compos. Mater., vol. 11, Oct. 1977, pp. 366-377.

17. Fox, Richard L.: Optimization Methods for Engineering Design. Addison-Wesley Pub. Co., Inc., c.1971.

18. Hepler, A. K.; and Bangsund, E. L.: Technology Requirements for Advanced Earth Orbital Transportation Systems. Volume 2: Summary Report. NASA CR-2879, 1978.

19. Mikulus, Martin M., Jr.; Bush, Harold G.; and Rhodes, Marvin D.: Current Langley Research Center Studies on Buckling and Low-Velocity Impact of Composite Panels. Third Conference on Fibrous Composites in Flight Vehicle Design - Part II. NASA TM X-3377, 1976, pp. 633-663.

20. Jackson, L. Robert: Multiwall TPS. Recent Advances in Structures for Hypersonic Flight. NASA CP-2065, 1978, pp. 671-706.

21. Arnquist, J. L.; and Hepler, A. K.: Development of Brazed René 41 Honeycomb Structure. 19th Structures, Structural Dynamics and Materials Conference, Apr. 1978, pp. 132-146. (Available as AIAA Paper 78-481.)

22. Whetstone, W. D.: SPAR Structural Analysis System Reference Manual - System Level 11. Volume 1: Program Execution. NASA CR-145098-1, 1977.

23. Harris, Robert S., Jr.; and Davidson, John R.: An Analysis of Exact and Approximate Equations for the Temperature Distribution in an Insulated Thick Skin Subjected to Aerodynamic Heating. NASA TN D-519, 1961.

24. Jones, Robert M.: Mechanics of Composite Materials. McGraw-Hill Book Co., c.1975.

TABLE I.- THERMAL PROPERTIES USED FOR OPTIMIZATION STUDIES OF INSULATED PANELS

Material	k		c		ρ		T_a	
	W/m-^{o}C	Btu/in-sec-^{o}F	J/kg-^{o}C	Btu/lbm-^{o}F	kg/m^3	lbm/in^3	K	^{o}F
Insulation	0.181	2.42×10^{-6}	1200	0.291	144	0.00521	----	----
Graphite/polyimide	2.30	3.08×10^{-5}	1297	.310	1550	.056	533	500
Graphite/epoxy	1.64	2.20×10^{-5}	962	.230	1550	.056	450	350
Boron/aluminum	67.8	9.07×10^{-4}	1397	.334	2712	.098	589	600
Aluminum	234	3.13×10^{-3}	920	.220	2770	.100	450	350
Titanium	9.49	1.27×10^{-4}	565	.135	4429	.160	589	600
René 41	28.4	3.80×10^{-4}	1260	.302	8249	.298	1089	1500
Carbon/carbon	6.56	8.78×10^{-5}	1380	.330	1439	.052	1644	2500
Lockalloy	167	2.23×10^{-3}	2050	.490	2090	.0756	700	800

TABLE II.- MECHANICAL PROPERTIES OF STRUCTURAL MATERIALS USED FOR OPTIMIZATION STUDIES OF INSULATED PANELS

Property		Material							
		Graphite/polyimide		Graphite/epoxy		Boron/aluminum		Aluminum	
Symbol	Unit	RT	533 K (500° F)	RT	450 K (350° F)	RT	589 K (600° F)	RT	450 K (350° F)
E_1	GPa (lbf/in^2)	133 (19.3×10^6)	133 (19.3×10^6)	155 (22.5×10^6)	155 (22.5×10^6)	200 (29×10^6)	205 (29.7×10^6)	73.1 (10.6×10^6)	69.6 (10.1×10^6)
E_2	GPa (lbf/in^2)	9.10 (1.32×10^6)	4.14 (0.6×10^6)	8.83 (1.28×10^6)	5.58 (0.81×10^6)	27.6 (4×10^6)	20.5 (2.98×10^6)	---- (----)	---- (----)
ν_1		0.37	0.51	0.30	0.23	0.27	0.21	0.33	0.33
G	GPa (lbf/in^2)	5.58 (0.81×10^6)	4.41 (0.64×10^6)	5.10 (0.74×10^6)	0.55 (0.08×10^6)	15.5 (2.25×10^6)	7.03 (1.02×10^6)	---- (----)	---- (----)
α_1	$^oC^{-1}$ ($^oF^{-1}$)	-0.68×10^{-6} (-0.38×10^{-6})	0.14×10^{-6} (0.08×10^{-6})	-0.23×10^{-6} (-0.13×10^{-6})	-0.13×10^{-6} (-0.07×10^{-6})	6.08×10^{-6} (3.38×10^{-6})	7.4×10^{-6} (4.1×10^{-6})	22.8×10^{-6} (12.65×10^{-6})	24.8×10^{-6} (13.8×10^{-6})
α_2	$^oC^{-1}$ ($^oF^{-1}$)	27×10^{-6} (15×10^{-6})	45×10^{-6} (25×10^{-6})	30.4×10^{-6} (18.9×10^{-6})	78.7×10^{-6} (43.7×10^{-6})	1.75 (9.7×10^{-6})	23.2×10^{-6} (12.9×10^{-6})	---- (----)	---- (----)
X_T	GPa (lbf/in^2)	1.09 (157 400)	1.02 (147 300)	1.11 (161 000)	1.03 (150 000)	1.41 (205 000)	1.17 (169 000)	0.40 (58 000)	0.32 (46 400)
X_C	MPa (lbf/in^2)	-867 (-125 800)	-450 (-65 200)	-970 (-141 000)	-848 (-123 000)	-2530 (-367 000)	-1972 (-286 000)	---- (----)	---- (----)
Y_T	MPa (lbf/in^2)	16.5 (2390)	6.62 (960)	35.8 (5190)	21.0 (3040)	162 (23 500)	144 (20 900)	---- (----)	---- (----)
Y_C	MPa (lbf/in^2)	-109 (-15 790)	-87.8 (-12 730)	-170 (-24 700)	-119 (-17 300)	-292 (-42 400)	-214 (-31 100)	---- (----)	---- (----)
S	MPa (lbf/in^2)	93.8 (13 600)	53.1 (7700)	57.9 (8400)	25.9 (3760)	93.1 (13 500)	27.9 (4050)	---- (----)	---- (----)
ρ	kg/m^3 (lbm/in^3)	1550 (0.056)	1550 (0.056)	1550 (0.056)	1550 (0.056)	2710 (0.098)	2710 (0.098)	2768 (0.100)	2768 (0.100)

TABLE II.- Concluded

Property		Material							
		Titanium		Rene 41		Carbon/carbon		Lockalloy	
Symbol	Unit	RT	589 K (600° F)	RT	1089 K (1500° F)	RT	1644 K (2500° F)	RT	700 K (800° F)
E_1	GPa (lbf/in^2)	114 (16.5×10^6)	103 (15×10^6)	212 (30.8×10^6)	117 (16.9×10^6)	13.8 (2×10^6)	20.7 (3×10^6)	186 (27×10^6)	110 (16×10^6)
E_2	GPa (lbf/in^2)	---- (----)	---- (----)	---- (----)	---- (----)	10.3 (1.5×10^6)	13.8 (2×10^6)	---- (----)	---- (----)
ν_1		0.30	0.30	0.30	0.30	0.19	0.19	0.14	0.14
G	GPa (lbf/in^2)	---- (----)	---- (----)	---- (----)	---- (----)	7.60 (1.1×10^6)	7.60 (1.1×10^6)	---- (----)	---- (----)
α_1	$^oC^{-1}$ ($^oF^{-1}$)	9.5×10^{-6} (5.3×10^{-6})	10.4×10^{-6} (5.8×10^{-6})	11.8×10^{-6} (6.55×10^{-6})	15.2×10^{-6} (8.43×10^{-6})	3.1×10^{-6} (1.7×10^{-6})	3.1×10^{-6} (1.7×10^{-6})	17.6×10^{-6} (9.8×10^{-6})	17.6×10^{-6} (9.8×10^{-6})
α_2	$^oC^{-1}$ ($^oF^{-1}$)	---- (----)	---- (----)	---- (----)	---- (----)	3.1×10^{-6} (1.7×10^{-6})	3.1×10^{-6} (1.7×10^{-6})	---- (----)	---- (----)
X_T	GPa (lbf/in^2)	1.09 (155 000)	0.70 (101 500)	0.98 (142 000)	0.56 (81 000)	0.059 (8500)	0.069 (9700)	0.303 (44 000)	0.17 (25 000)
X_C	MPa (lbf/in^2)	---- (----)	---- (----)	---- (----)	---- (----)	-79.3 (-11 500)	-126 (-18 300)	---- (----)	---- (----)
Y_T	MPa (lbf/in^2)	---- (----)	---- (----)	---- (----)	---- (----)	31.0 (4500)	40.7 (5900)	---- (----)	---- (----)
Y_C	MPa (lbf/in^2)	---- (----)	---- (----)	---- (----)	---- (----)	-82.0 (-11 900)	-82.0 (-11 900)	---- (----)	---- (----)
S	MPa (lbf/in^2)	---- (----)	---- (----)	---- (----)	---- (----)	26.5 (3850)	26.5 (3850)	---- (----)	---- (----)
ρ	kg/m^3 (lbm/in^3)	4429 (0.16)	4429 (0.16)	8248 (0.298)	8248 (0.298)	1439 (0.052)	1439 (0.052)	2093 (0.0756)	2093 (0.0756)

TABLE III.- LOWER LIMITS ON THICKNESSES USED IN CALCULATIONS

Material	Minimum thickness	
	mm	in.
Insulation	3.810	0.15
Graphite/polyimide	.076	*.003
Graphite/epoxy	.076	*.003
Boron/aluminum	.076	*.003
Aluminum	.610	.024
Titanium	.610	.024
Rene 41	.762	.030
Carbon/carbon	.031	*.012
Lockalloy	.813	.032

*Ply thickness.

TABLE IV.- CHARACTERISTICS OF MINIMUM-MASS INSULATED PANELS FOR VARIOUS STRUCTURAL MATERIALS

(a) T_{peak} = 1089 K (1500° F); $N_x = N_y = 0$; $N_{xy} = 0$

Material	Total mass		Maximum temperature		Time of maximum temperature, sec	Maximum stress ratio	Time of maximum stress ratio, sec
	kg/m^2	lbm/ft^2	K	°F			
Graphite/polyimide	11.82	2.42	533	500	2000	0	----
Graphite/epoxy	15.87	3.25	450	350	2800	.01	0
Boron/aluminum	10.20	2.09	389	600	2000	.10	2000
Aluminum	16.06	3.29	450	350	2800	0	----
Titanium	11.82	2.42	589	600	2000	0	----
René 41	6.30	1.29	1078	1480	800	0	----
Lockalloy	7.82	1.60	700	800	1600	0	----
Carbon/carbon	1.76	.36	1078	1480	800	0	----

(b) T_{peak} = 1089 K (1500° F); $N_x = N_y$ = -525 kN/m (-3000 lbf/in.); N_{xy} = 350 kN/m (2000 lbf/in.)

Material	Total mass		Maximum temperature		Time of maximum temperature, sec	Maximum stress ratio	Time of maximum stress ratio, sec
	kg/m^2	lbm/ft^2	K	°F			
Graphite/polyimide	11.96	2.45	533	500	2000	0.65	2000
Graphite/epoxy	15.87	3.25	450	350	2800	.87	2800
Boron/aluminum	11.13	2.28	583	590	1600	1.00	1600
Aluminum	17.58	3.60	450	350	2400	1.00	2400
Titanium	13.18	2.70	589	600	2000	.98	2000
René 41	11.72	2.40	1078	1480	800	1.00	800
Lockalloy	11.72	2.40	567	560	1600	1.00	1600
Carbon/carbon	20.41	4.18	1081	1486	800	1.00	2400

TABLE IV.- Continued

(c) T_{peak} = 1089 K (1500° F); $N_x = N_y$ = -1.05 MN/m (-6000 lbf/in.); N_{xy} = 700 kN/m (4000 lbf/in.)

Material	Total mass		Maximum temperature		Time of maximum temperature, sec	Maximum stress ratio	Time of maximum stress ratio, sec
	kg/m^2	lbm/ft^2	K	°F			
Graphite/polyimide	13.28	2.72	533	500	2000	0.76	2000
Graphite/epoxy	16.60	3.40	450	350	2800	1.00	2800
Boron/aluminum	14.84	3.04	522	480	1600	1.00	1600
Aluminum	21.53	4.41	450	350	2000	1.00	2000
Titanium	16.45	3.37	584	592	2000	1.00	2000
René 41	23.39	4.79	1078	1480	800	1.00	800
Lockalloy	16.55	3.39	503	445	1600	1.00	1600
Carbon/carbon	41.35	8.47	1076	1477	800	1.00	2800

(d) T_{peak} = 1089 K (1500° F); $N_x = N_y$ = -1.58 MN/m (-9000 lbf/in.); N_{xy} = 1.05 MN/m (6000 lbf/in.)

Material	Total mass		Maximum temperature		Time of maximum temperature, sec	Maximum stress ratio	Time of maximum stress ratio, sec
	kg/m^2	lbm/ft^2	K	°F			
Graphite/polyimide	13.96	2.86	530	494	2000	1.00	2000
Graphite/epoxy	18.02	3.69	450	350	2400	.92	2400
Boron/aluminum	16.70	3.42	494	429	2000	1.00	2000
Aluminum	29.29	6.00	384	232	2800	1.00	2800
Titanium	20.36	4.17	548	527	2000	1.00	2000
René 41	35.06	7.18	1078	1480	800	1.00	800
Lockalloy	21.53	4.41	475	395	1600	1.00	1600
Carbon/carbon	62.50	12.80	1018	1373	800	1.00	2800

TABLE IV.- Continued

(e) T_{peak} = 1089 K (1500° F); $N_x = N_y$ = -2.10 MN/m (-12 000 lbf/in.); N_{xy} = 1.40 MN/m (8000 lbf/in.)

Material	Total mass		Maximum temperature		Time of maximum temperature, sec	Maximum stress ratio	Time of maximum stress ratio, sec
	kg/m^2	lbm/ft^2	K	°F			
Graphite/polyimide	17.53	3.59	498	437	2000	1.00	2000
Graphite/epoxy	20.07	4.11	440	340	2400	.75	2400
Boron/aluminum	19.48	3.99	499	438	1600	1.00	1600
Aluminum	33.88	6.94	384	232	2400	1.00	2400
Titanium	24.17	4.95	570	536	1600	1.00	1600
René 41	46.72	9.57	1078	1480	800	1.00	800
Lockalloy	26.80	5.49	456	360	1600	1.00	1600
Carbon/carbon	82.61	16.92	924	1204	800	1.00	3600

(f) T_{peak} = 1089 K (1500° F); $N_x = N_y$ = -2.63 MN/m (-15 000 lbf/in.); N_{xy} = 1.75 MN/m (10 000 lbf/in.)

Material	Total mass		Maximum temperature		Time of maximum temperature, sec	Maximum stress ratio	Time of maximum stress ratio, sec
	kg/m^2	lbm/ft^2	K	°F			
Graphite/polyimide	21.73	4.45	417	290	2000	1.00	2000
Graphite/epoxy	24.90	5.10	450	350	2400	.89	0
Boron/aluminum	22.36	4.58	517	370	2000	1.00	2000
Aluminum	38.08	7.80	432	318	2000	1.00	2000
Titanium	28.12	5.76	555	540	1600	1.00	1600
René 41	58.44	11.97	1078	1480	800	1.00	800
Lockalloy	33.40	6.84	505	449	1600	1.00	1600
Carbon/carbon	96.28	19.72	889	1140	1200	1.00	0

TABLE IV.- Continued

(g) T_{peak} = 1533 K (2300° F); $N_x = N_y = 0$; $N_{xy} = 0$

Material	Total mass		Maximum temperature		Time of maximum temperature, sec	Maximum stress ratio	Time of maximum stress ratio, sec
	kg/m^2	lbm/ft^2	K	°F			
Graphite/polyimide	15.77	3.23	533	500	2400	0	----
Graphite/epoxy	19.53	4.00	450	350	3600	.06	0
Boron/aluminum	13.57	2.78	589	600	2400	.13	2400
Aluminum	20.65	4.23	450	350	3600	0	----
Titanium	15.53	3.18	589	600	2400	0	----
René 41	11.03	2.26	1089	1500	1200	0	----
Lockalloy	10.89	2.23	700	800	2000	0	----
Carbon/carbon	1.76	.36	1515	2268	800	.96	0

(h) T_{peak} = 1533 K (2300° F); $N_x = N_y$ = -525 kN/m (-3000 lbf/in.); N_{xy} = 350 kN/m (2000 lbf/in.)

Material	Total mass		Maximum temperature		Time of maximum temperature, sec	Maximum stress ratio	Time of maximum stress ratio, sec
	kg/m^2	lbm/ft^2	K	°F			
Graphite/polyimide	15.77	3.23	533	500	2400	0.26	0
Graphite/epoxy	19.72	4.04	450	350	3600	.93	3600
Boron/aluminum	14.89	3.05	560	548	2400	1.00	2400
Aluminum	21.43	4.39	450	350	3200	1.00	3200
Titanium	16.40	3.36	589	600	2400	1.00	2400
René 41	15.28	3.13	1046	1423	1200	1.00	1200
Lockalloy	13.38	2.74	656	720	1600	1.00	1600
Carbon/carbon	20.41	4.18	1520	2277	800	1.00	0

TABLE IV.- Continued

(i) T_{peak} = 1533 K (2300° F); $N_x = N_y$ = -1.05 MN/m (-6000 lbf/in.); N_{xy} = 700 kN/m (4000 lbf/in.)

Material	Total mass		Maximum temperature		Time of maximum temperature, sec	Maximum stress ratio	Time of maximum stress ratio, sec
	kg/m^2	lbm/ft^2	K	°F			
Graphite/polyimide	16.21	3.32	533	500	2400	0.94	2400
Graphite/epoxy	21.04	4.31	440	332	4000	1.00	4000
Boron/aluminum	16.80	3.44	560	549	2000	.91	2000
Aluminum	25.10	5.14	450	350	2800	1.00	2800
Titanium	20.94	4.29	589	600	2000	.83	2000
René 41	24.17	4.95	713	824	2000	1.00	2000
Lockalloy	18.55	3.80	563	554	2000	1.00	2000
Carbon/carbon	41.35	8.47	1513	2264	800	1.00	0

(j) T_{peak} = 1533 K (2300° F); $N_x = N_y$ = -1.58 MN/m (-9000 lbf/in.); N_{xy} = 1.05 MN/m (6000 lbf/in.)

Material	Total mass		Maximum temperature		Time of maximum temperature, sec	Maximum stress ratio	Time of maximum stress ratio, sec
	kg/m^2	lbm/ft^2	K	°F			
Graphite/polyimide	18.06	3.70	533	500	2000	0.06	0
Graphite/epoxy	21.58	4.42	450	350	3200	.95	3200
Boron/aluminum	19.24	3.94	516	470	2000	1.00	2000
Aluminum	30.66	6.28	426	307	2800	1.00	2800
Titanium	23.19	4.75	589	600	2000	1.00	2000
René 41	31.64	6.48	783	950	1600	1.00	1600
Lockalloy	23.63	4.84	489	420	2000	1.00	2000
Carbon/carbon	62.40	12.78	1422	2100	800	1.00	0

TABLE IV.- Concluded

(k) T_{peak} = 1533 K (2300° F); $N_x = N_y$ = -2.10 MN/m (-12 000 lbf/in.); N_{xy} = 1.40 MN/m (8000 lbf/in.)

Material	Total mass		Maximum temperature		Time of maximum temperature, sec	Maximum stress ratio	Time of maximum stress ratio, sec
	kg/m^2	lbm/ft^2	K	°F			
Graphite/polyimide	19.68	4.03	529	492	2000	1.00	2000
Graphite/epoxy	25.44	5.21	425	305	3600	1.00	0
Boron/aluminum	22.02	4.51	499	438	2000	1.00	2000
Aluminum	35.05	7.18	448	346	2400	1.00	2400
Titanium	27.05	5.54	581	586	2000	1.00	2000
René 41	38.96	7.98	709	817	1600	1.00	1600
Lockalloy	28.51	5.84	474	394	2000	1.00	2000
Carbon/carbon	82.56	16.91	1277	1839	1200	1.00	0

(l) T_{peak} = 1533 K (2300° F); $N_x = N_y$ = -2.63 MN/m (-15 000 lbf/in.); N_{xy} = 1.75 MN/m (10 000 lbf/in.)

Material	Total mass		Maximum temperature		Time of maximum temperature, sec	Maximum stress ratio	Time of maximum stress ratio, sec
	kg/m^2	lbm/ft^2	K	°F			
Graphite/polyimide	25.00	5.12	454	358	2400	1.00	2000
Graphite/epoxy	29.34	6.01	433	319	2800	1.00	0
Boron/aluminum	25.10	5.14	459	367	2400	1.00	2400
Aluminum	41.06	8.41	412	282	2400	1.00	2400
Titanium	30.71	6.29	532	498	2000	1.00	2000
René 41	49.95	10.23	847	1065	1600	1.00	1600
Lockalloy	33.79	6.92	463	373	2000	1.00	2000
Carbon/carbon	96.28	19.72	1220	1736	1200	1.00	0

TABLE V.- OPTIMUM MASS OF INSULATED PANELS FOR VARIOUS VALUES OF HEATING INTENSITY AND DURATION

[$N_x = N_y = -700$ kN/m (-4000 lbf/in.); $N_{xy} = 525$ kN/m (3000 lbf/in.)]

Material	T_{peak} = 1089 K (1500° F)				T_{peak} = 1533 K (2300° F)			
	τ_f = 1500 sec		τ_f = 2000 sec		τ_f = 1500 sec		τ_f = 2000 sec	
	kg/m^2	lbm/ft^2	kg/m^2	lbm/ft^2	kg/m^2	lbm/ft^2	kg/m^2	lbm/ft^2
Graphite/polyimide	11.57	2.37	12.01	2.46	14.16	2.90	15.23	3.12
Graphite/epoxy	15.14	3.10	15.97	3.27	18.31	3.75	20.16	4.13
Boron/aluminum	*13.72	*2.81	15.14	3.10	*16.36	*3.35	19.33	3.96
Aluminum	18.16	3.72	19.19	3.93	21.43	4.39	23.00	4.71
Titanium	*14.26	*2.92	14.45	2.96	16.80	3.44	18.46	3.78
Rene' 41	*16.70	*3.42	*16.75	*3.43	-----	----	-----	----
Carbon/carbon	*30.27	*6.20	*30.27	*6.20	*30.27	*6.20	*30.27	*6.20
Lockalloy	*13.23	*2.71	*14.79	*3.03	*15.48	*3.17	*16.01	*3.28

*Temperature response less than allowable value.

TABLE VI.- EFFECT OF TIME-DEPENDENT LOADS ON DESIGNS OF INSULATED PANELS

Material	Type of load	Mass		Maximum temperature		Time of maximum temperature, sec	Maximum stress ratio	Time of maximum stress ratio, sec
		kg/m^2	lbm/ft^2	K	^oF			
Graphite/ epoxy*	Constant	16.60	3.40	450	350	2800	1.00	2800
	Time dependent	16.40	3.36	450	350	2800	0.87	1600
Titanium**	Constant	20.36	4.17	548	527	2000	1.00	2000
	Time dependent	20.21	4.14	558	544	2000	1.00	1600

*$N_x = N_y = -1.05$ MN/m (-6000 lbf/in.); $N_{xy} = 700$ kN/m (4000 lbf/in.); $\tau_f = 2000$ sec; $T_{peak} = 1089$ K (1500° F).

**$N_x = N_y = -1.58$ MN/m (-9000 lbf/in.); $N_{xy} = 1.05$ MN/m (6000 lbf/in.); $\tau_f = 2000$ sec; $T_{peak} = 1089$ K (1500° F).

TABLE VII.- EFFECT OF BACK-FACE RADIATION ON MAXIMUM STRUCTURAL TEMPERATURES

[Calculations for final designs corresponding to: $N_x = N_y = -1.58$ MN/m (-9000 lbf/in.); $N_{xy} = 1.05$ MN/m (6000 lbf/in.); $\tau_f = 2000$ sec; $T_{peak} = 1089$ K (1500° F)]

Material	Maximum temperature			
	Adiabatic back face		Radiating back face	
	K	°F	K	°F
Graphite/polyimide	530	494	453	355
Graphite/epoxy	450	350	393	248
Boron/aluminum	492	429	441	334
Aluminum	384	232	362	191
Titanium	548	527	451	352
René 41	1078	1480	1069	1464
Lockalloy	475	395	448	346
Carbon/carbon	1018	1373	963	1274

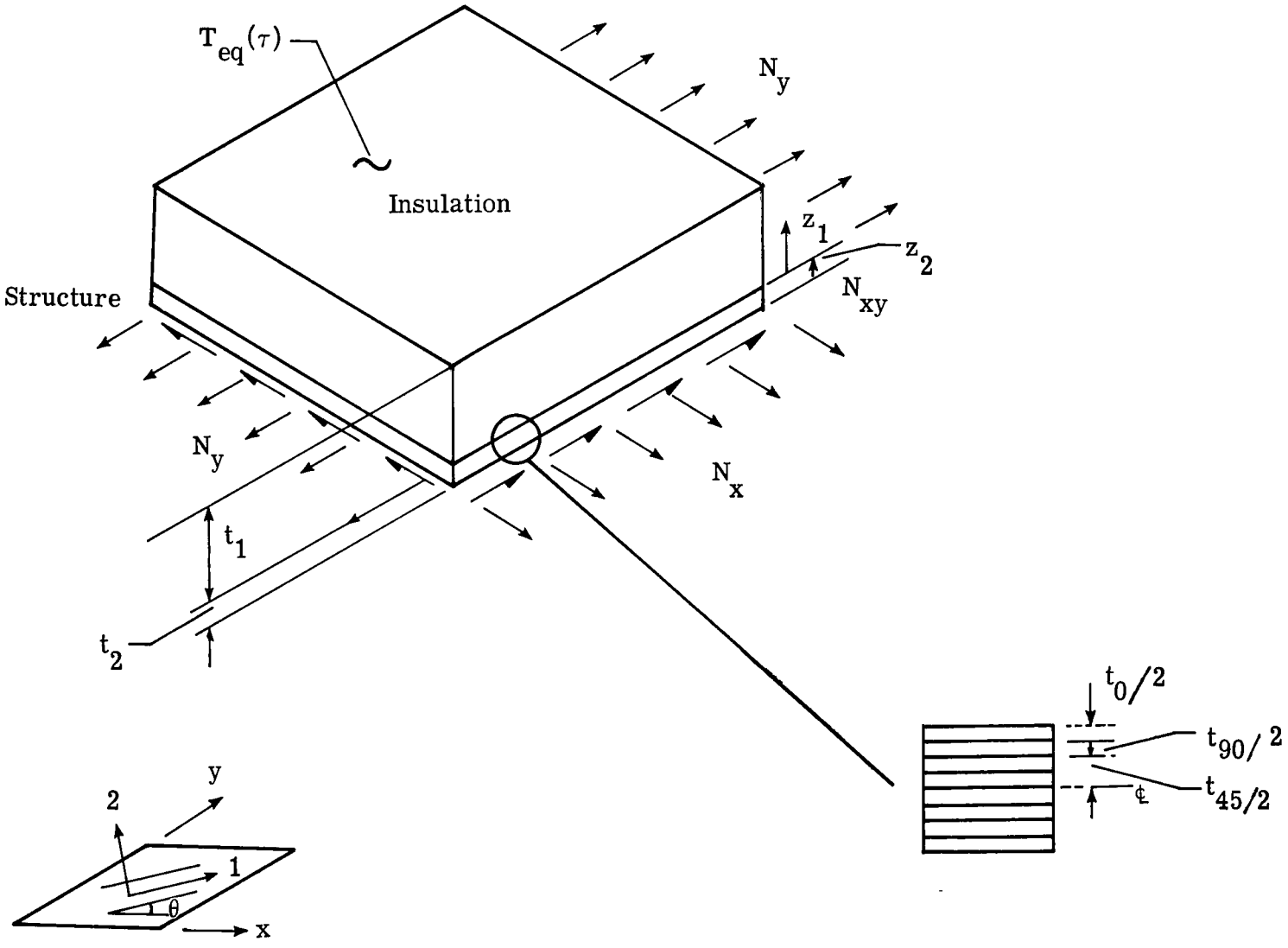

Lamina and laminate coordinates

Figure 1.- Insulated composite laminate.

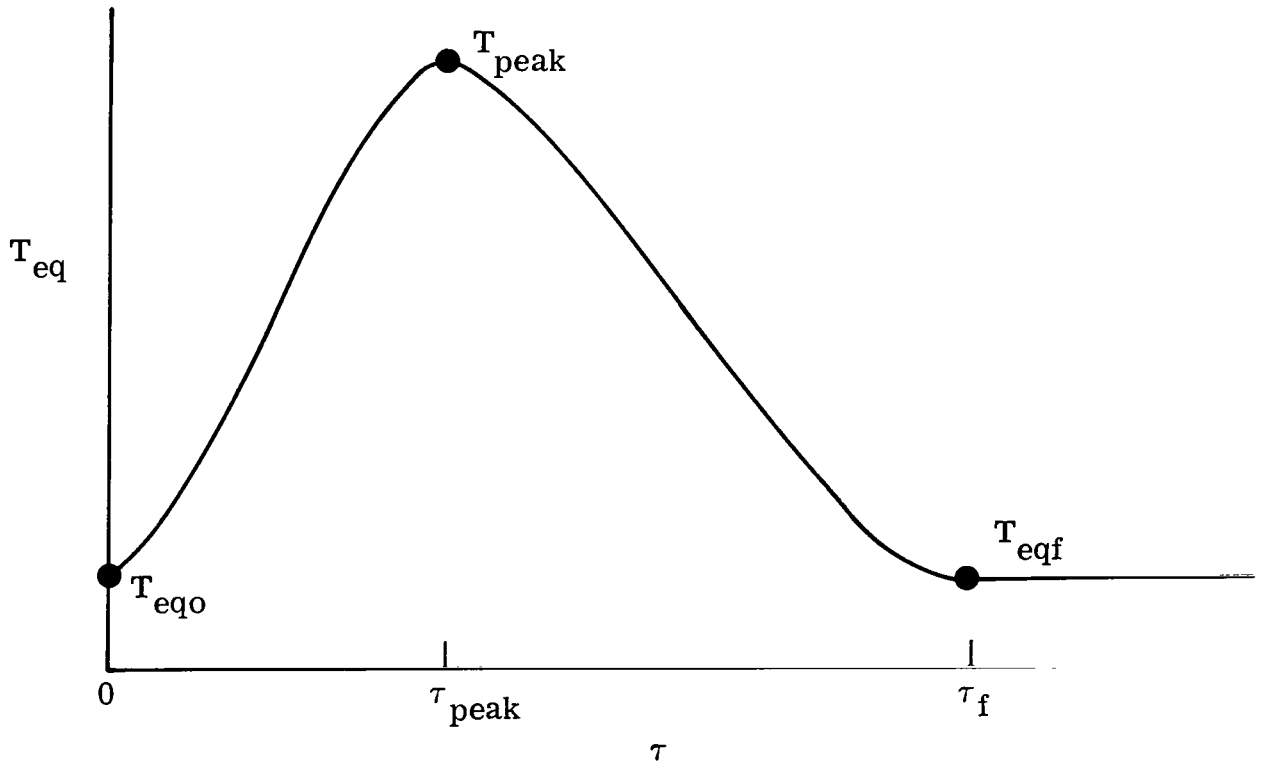

Figure 2.- Representation of outer surface temperature for insulated panel.

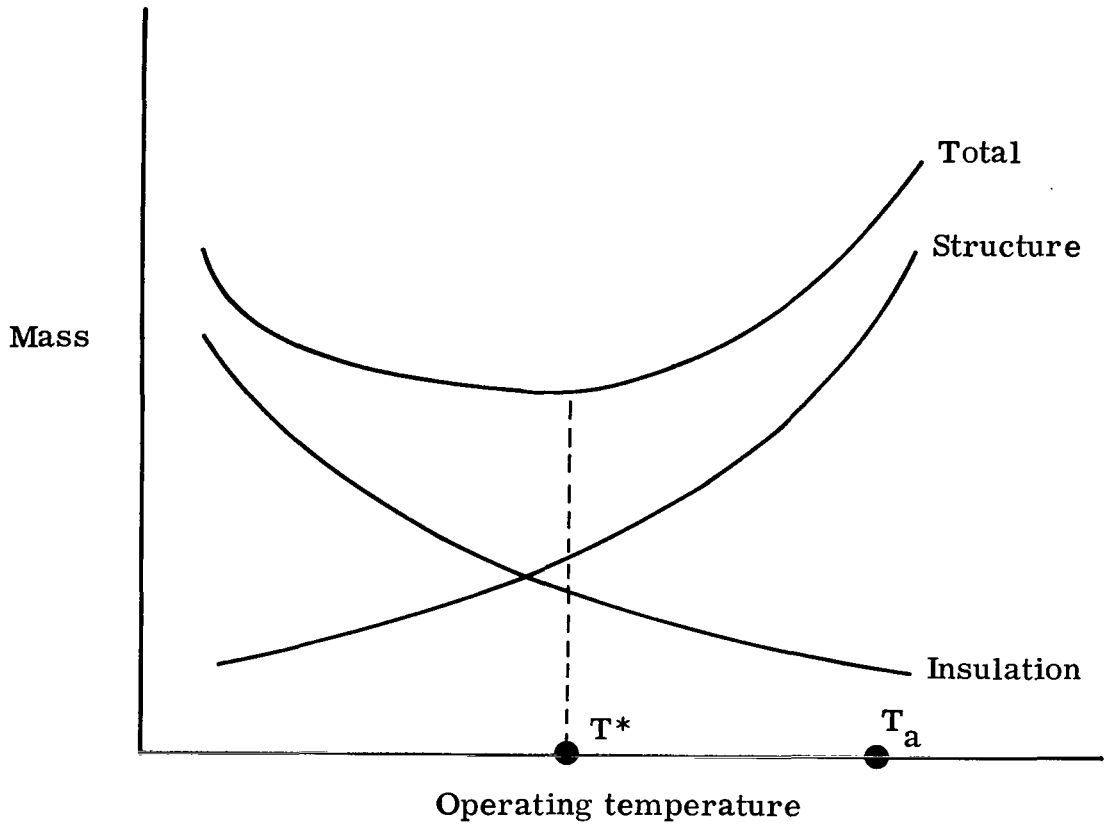

Figure 3.- Relationship between operating temperature and mass of insulated panel.

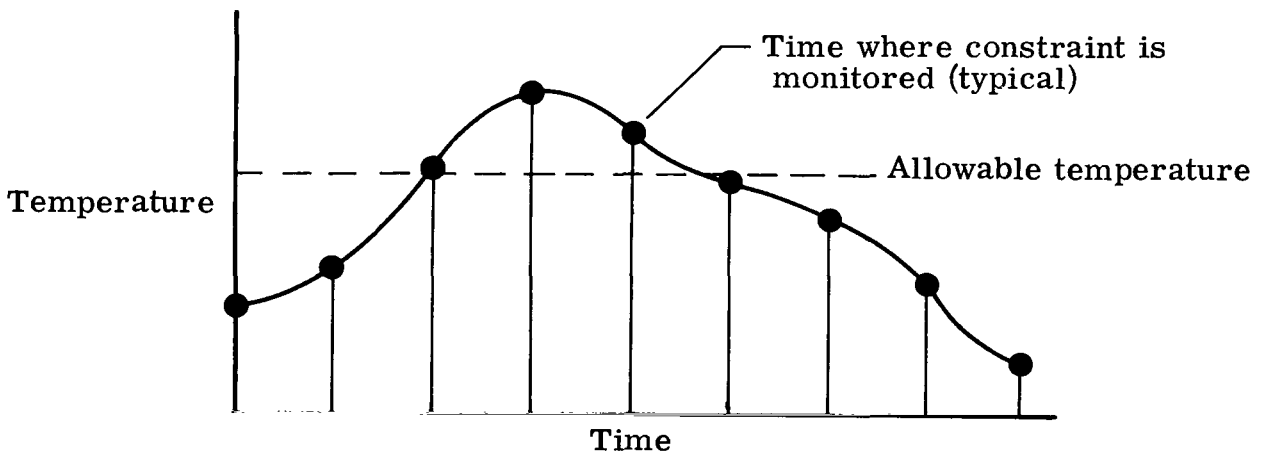

Figure 4.- Discrete-times approach for constraints on transient temperature response.

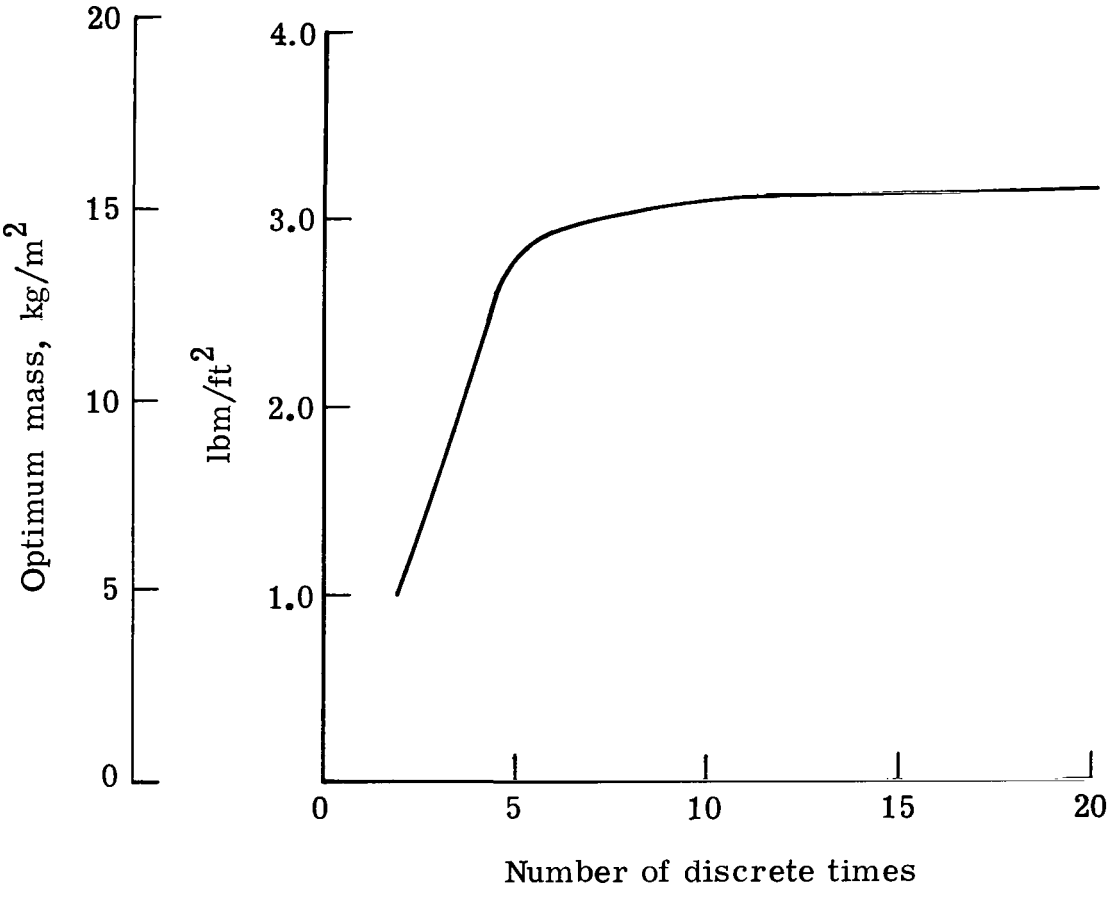

Figure 5.- Effect of number of discrete times on optimum mass of insulated Gr/E panel. $N_x = N_y = -700$ kN/m (-4000 lbf/in.); $N_{xy} = 525$ kN/m (3000 lbf/in.); $T_{peak} = 1089$ K (1500° F); $\tau_f = 1500$ sec.

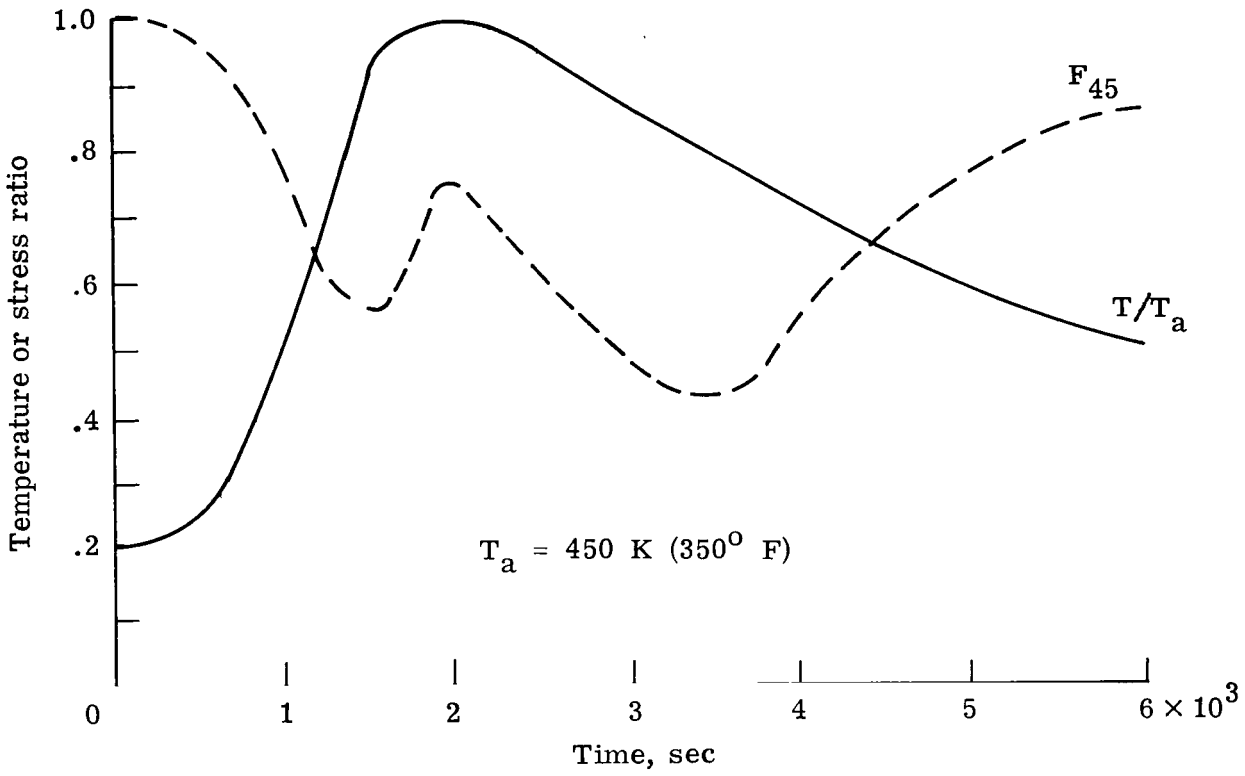

(a) $N_x = N_y = -700$ kN/m (-4000 lbf/in.); $N_{xy} = 525$ kN/m (3000 lbf/in.).

Figure 6.- Temperature and stress histories for final designs of insulated Gr/E panel (45° ply). T_{peak} = 1089 K (1500° F); τ_f = 1500 sec.

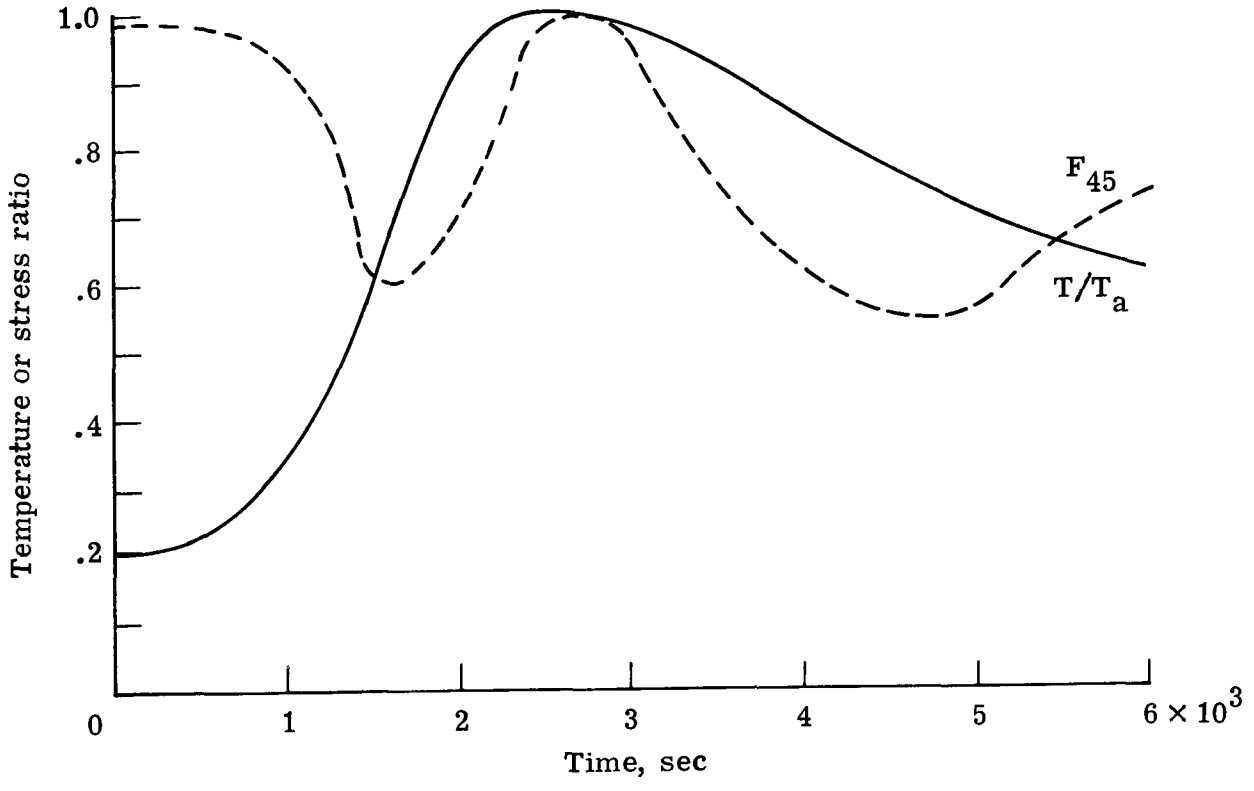

(b) $N_x = N_y = -1.05$ MN/m (-6000 lbf/in.); $N_{xy} = 700$ kN/m (4000 lbf/in.).

Figure 6.- Concluded.

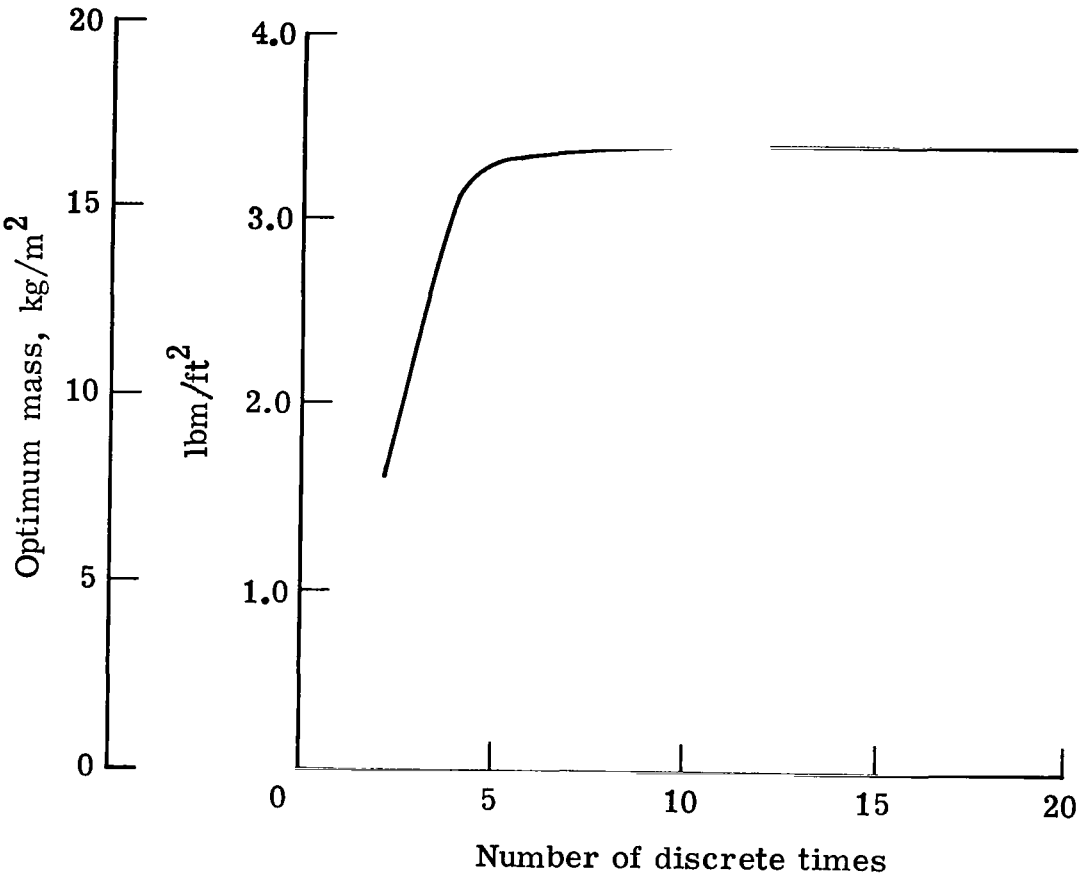

Figure 7.- Effect of number of discrete times on optimum mass of insulated Gr/E panel. $N_x = N_y = -1.05$ MN/m (-6000 lbf/in.); $N_{xy} = 700$ kN/m (4000 lbf/in.); $T_{peak} = 1089$ K (1500° F); $\tau_f = 1500$ sec.

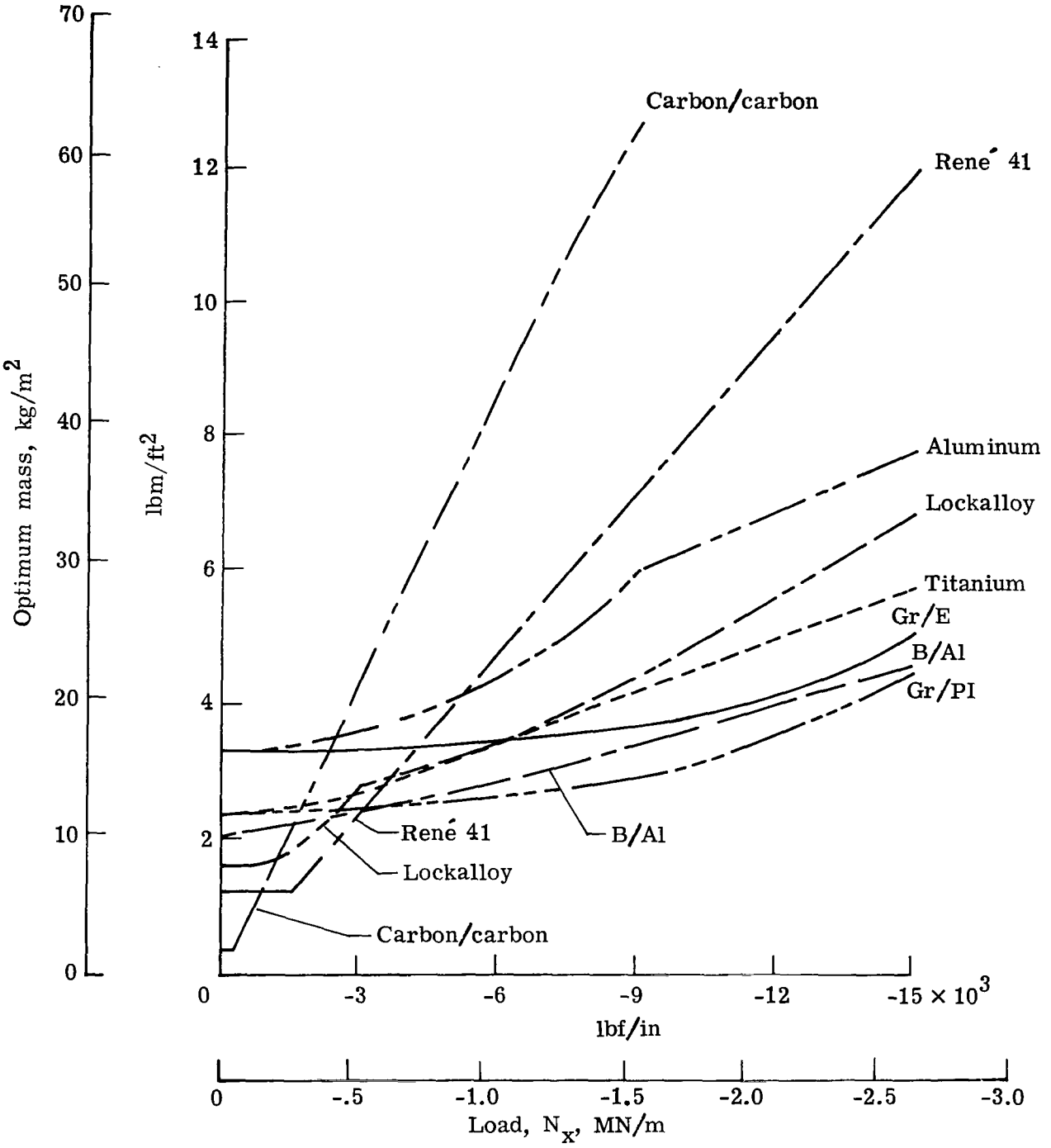

Figure 8.- Optimum mass of insulated panels. $N_y = N_x$; $N_{xy} = (2/3)N_x$; T_{peak} = 1089 K (1500° F).

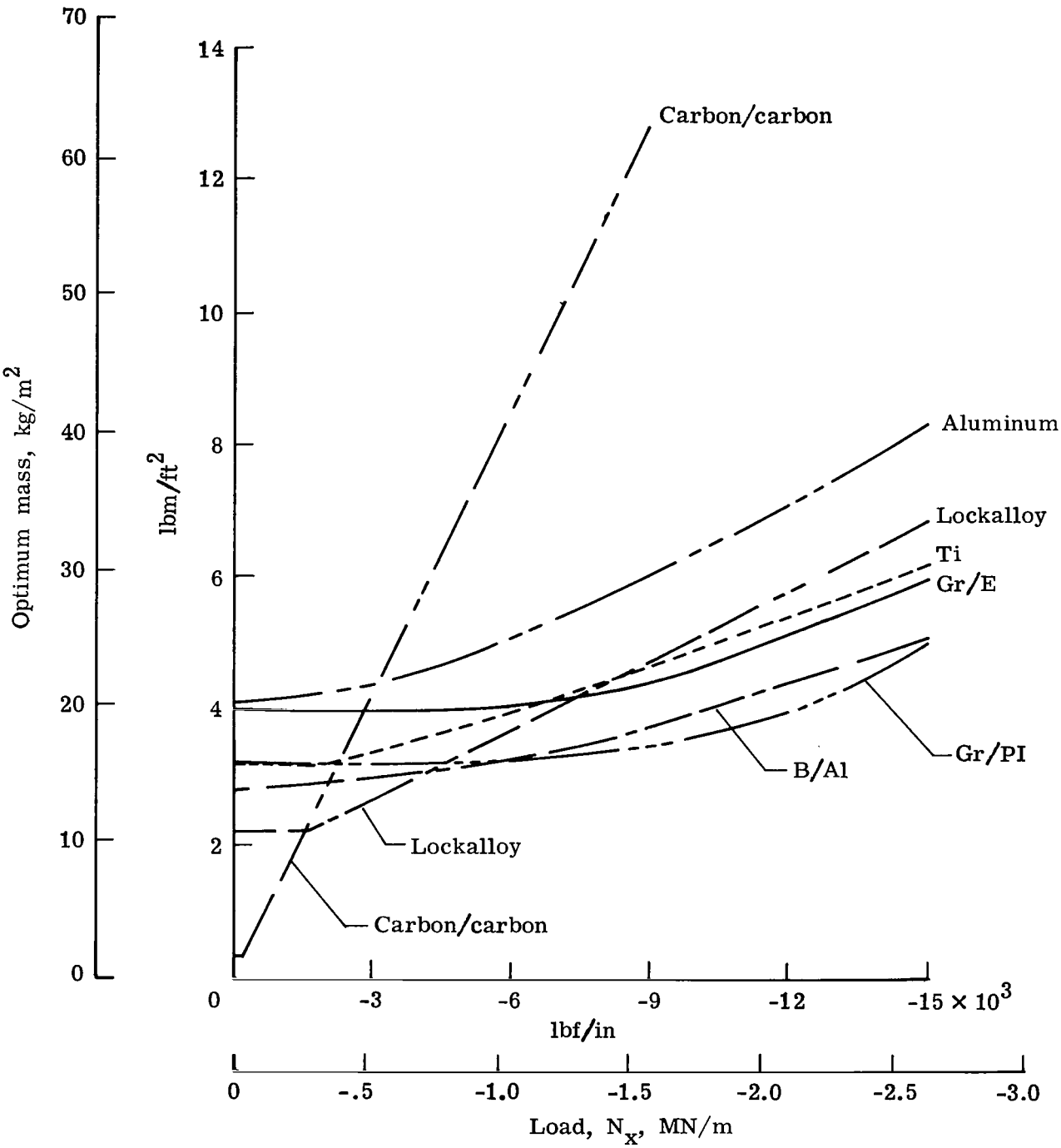

Figure 9.- Optimum mass of insulated panels. $N_x = N_y$; $N_{xy} = (2/3)N_x$; T_{peak} = 1533 K (2300° F).

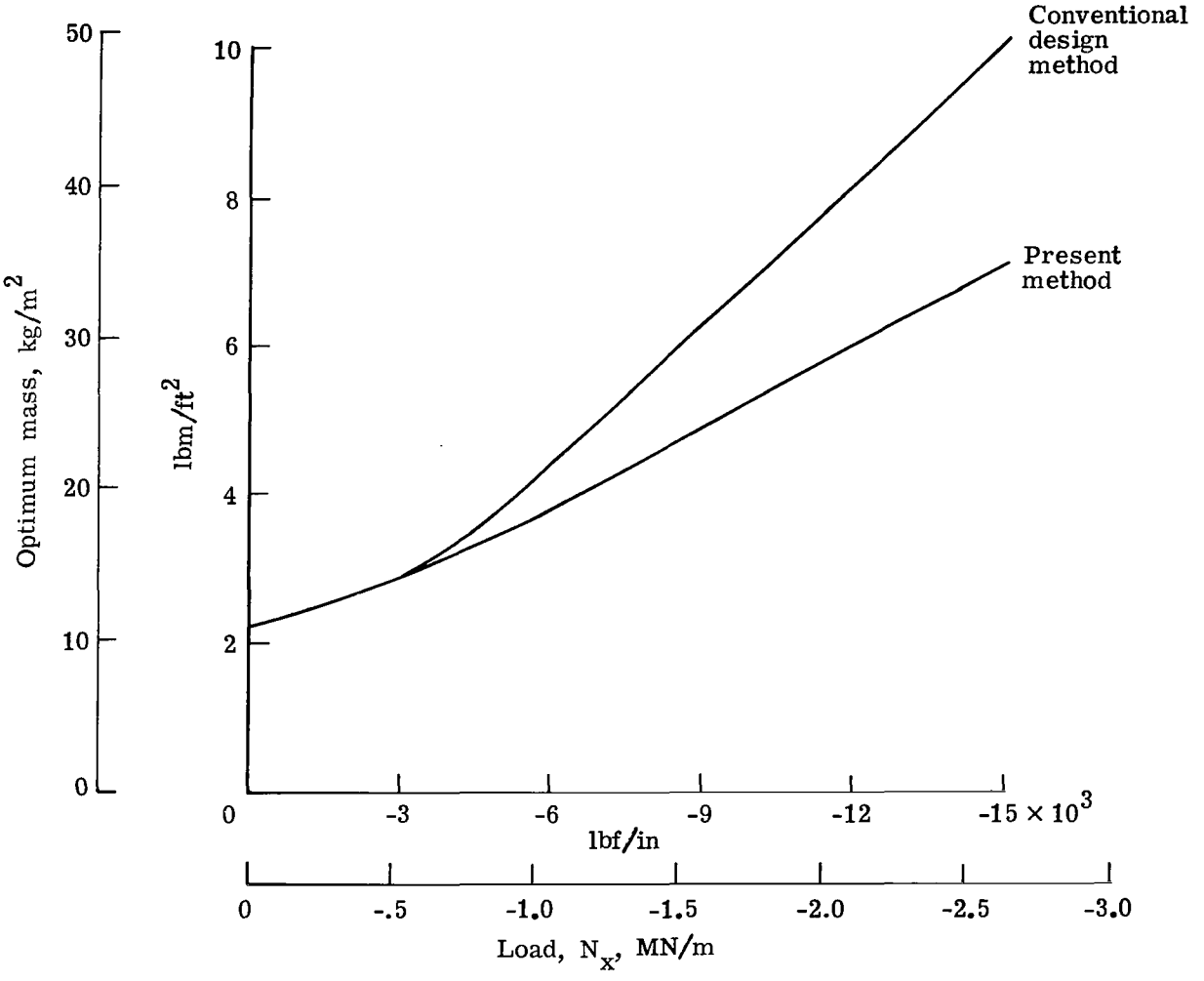

Figure 10.- Comparison of minimum mass from present method with conventional design based on operation at allowable temperature for Lockalloy. T_a = 700 K (800° F); T_{peak} = 1533 K (2300° F); τ_f = 2000 sec.

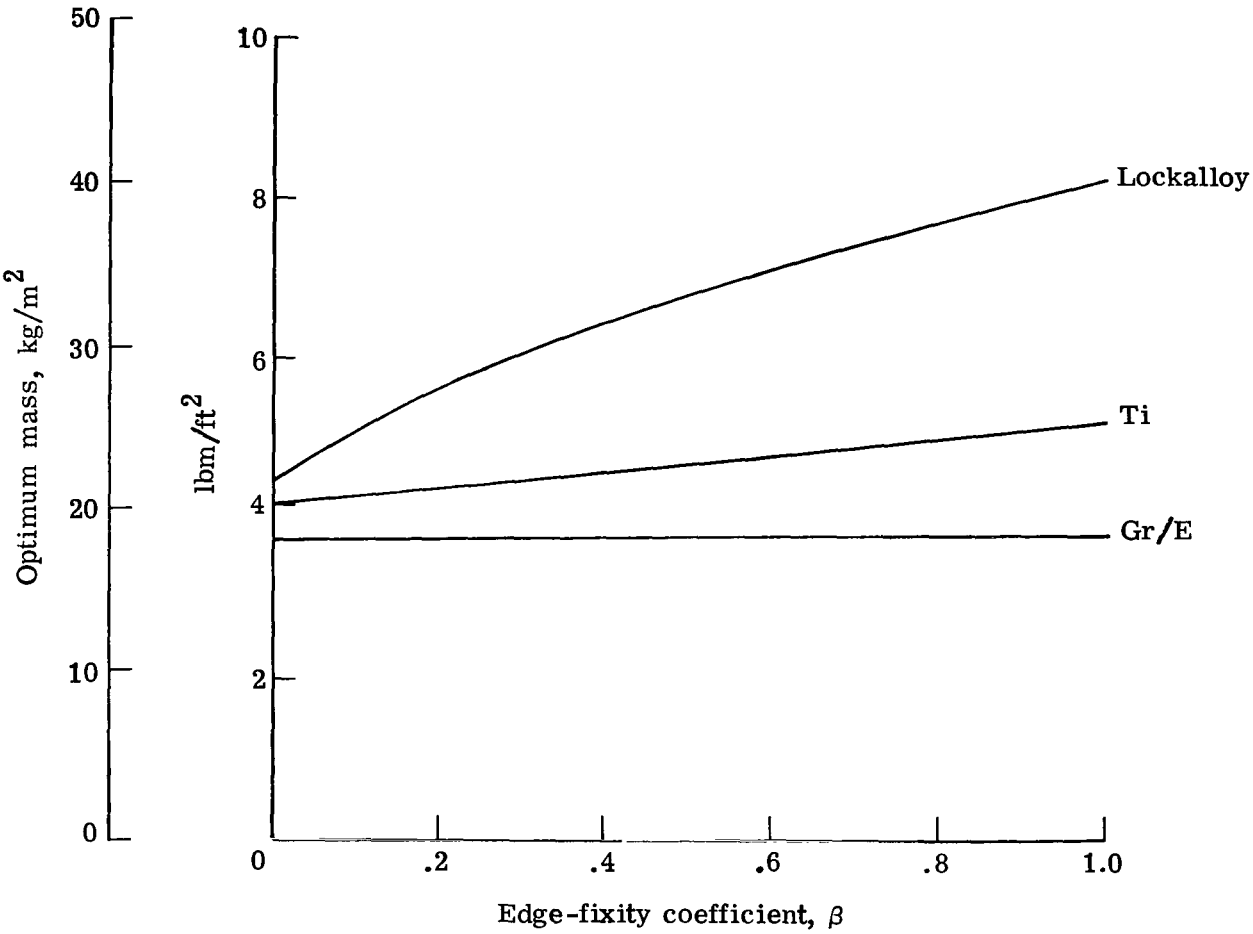

Figure 11.- Effect of restrained thermal expansion on mass of insulated panels. $N_x = N_y = -1.58$ MN/m (-9000 lbf/in.); $N_{xy} = 1.05$ MN/m (6000 lbf/in.); $T_{peak} = 1089$ K (1500° F); $\tau_f = 2000$ sec.

$$\begin{Bmatrix} N_x \\ N_y \\ N_{xy} \end{Bmatrix} = \begin{Bmatrix} N_x \\ N_y \\ N_{xy} \end{Bmatrix}_{max} F(\tau)$$

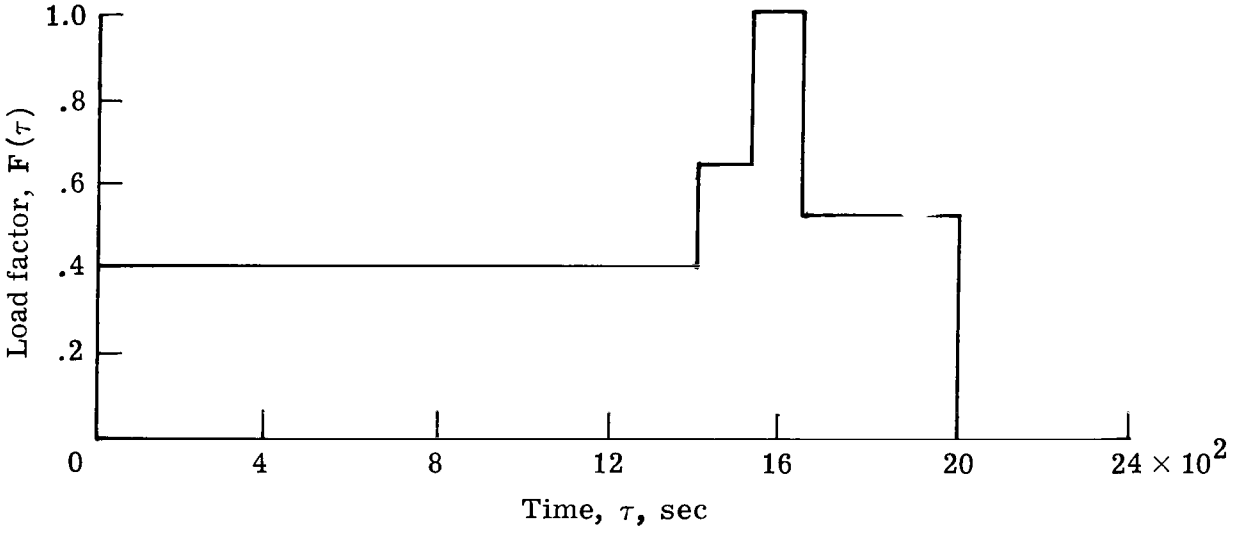

Figure 12.- Time-dependence of loading on insulated panel.

1. Report No.	2. Government Accession No.	3. Recipient's Catalog No.
NASA TP-1534		

4. Title and Subtitle	5. Report Date
PRELIMINARY DESIGN PROCEDURE FOR INSULATED STRUCTURES SUBJECTED TO TRANSIENT HEATING	December 1979
	6. Performing Organization Code
7. Author(s)	8. Performing Organization Report No.
Howard M. Adelman	L-13144
	10. Work Unit No.
9. Performing Organization Name and Address	506-53-53-02
NASA Langley Research Center Hampton, VA 23665	11. Contract or Grant No.
	13. Type of Report and Period Covered
12. Sponsoring Agency Name and Address	Technical Paper
National Aeronautics and Space Administration Washington, DC 20546	14. Sponsoring Agency Code

15. Supplementary Notes

16. Abstract

A procedure is described for obtaining minimum-mass designs of insulated structural panels loaded by a general set of inplane forces and a time-dependent temperature. Temperature and stress histories in the structure are given by closed-form solutions, and optimization of the insulation and structural thicknesses is performed by nonlinear mathematical programming techniques.

Design calculations are described to evaluate the structural efficiency of eight materials under combined heating and mechanical loads: graphite/polyimide, graphite/epoxy, boron/aluminum, titanium, aluminum, Rene 41, carbon/carbon, and Lockalloy. A study is also performed to assess the effect on design mass of intensity and duration of heating. Results indicate that an optimum structure may have a temperature response well below the recommended allowable temperature for the material. This suggests significant mass savings by lower temperature operation.

17. Key Words (Suggested by Author(s))	18. Distribution Statement
Insulated structures Structural design Structural optimization Transient heating Composite materials	Unclassified - Unlimited Subject Category 39

19. Security Classif. (of this report)	20. Security Classif. (of this page)	21. No. of Pages	22. Price*
Unclassified	Unclassified	50	$4.50

* For sale by the National Technical Information Service, Springfield, Virginia 22161

NASA-Langley, 1979

6 1 1U,D, 102279 S00903DS
DEPT OF THE AIR FORCE
AF WEAPONS LABORATORY
ATTN: TECHNICAL LIBRARY (SUL)
KIRTLAND AFB NM 87117